UNIVERSITY OF BIRMINGHAM

Sensitive detection of pre-integration intermediates of long terminal repeat retrotransposons in crop plants

Cho, Jungnam; Benoit, Matthias; Catoni, Marco; Drost, Hajk-Georg; Brestovitsky, Anna; Oosterbeek, Matthijs; Paszkowski, Jerzy

[Link to publication on Research at Birmingham portal](#)

1 **Title**

2 Sensitive detection of pre-integration intermediates of LTR retrotransposons in crop plants

3

4 **Authors**

5 Jungnam Cho[1,2,3,]*, Matthias Benoit[1], Marco Catoni[1,4], Hajk-Georg Drost[1], Anna Brestovitsky[1],

6 Matthijs Oosterbeek[5,6] and Jerzy Paszkowski[1,]*

7 [1]The Sainsbury Laboratory, University of Cambridge, Cambridge CB2 1LR, UK

8 [2]National Key Laboratory of Plant Molecular Genetics (NKLPMG), CAS Center for Excellence

9 in Molecular Plant Sciences, Institute of Plant Physiology and Ecology (SIPPE), 200032

10 Shanghai, P. R. China

11 [3]CAS-JIC Centre of Excellence for Plant and Microbial Science (CEPAMS), Chinese Academy

12 of Sciences, 200032 Shanghai, P. R. China

13 [4]School of Biosciences, University of Birmingham, Birmingham BI5 2TT, UK

14 [5]Laboratory of Molecular Biology, Wageningen University, Wageningen 6708PB, The

15 Netherlands

16 [6]Current address: Laboratory of Nematology, Wageningen University, Wageningen 6708PB,

17 The Netherlands

18 *Corresponding author

19

20 **Correspondence:**

21 Jungnam Cho jungnam.cho@slcu.cam.ac.uk and Jerzy Paszkowski

22 jerzy.paszkowski@slcu.cam.ac.uk

23

24 **Abstract**

25   **Retrotransposons have played an important role in the evolution of host**

26 **genomes[1,2]. Their impact is mainly deduced from the composition of DNA sequences that**

27 **have been fixed over evolutionary time[2]. Such studies provide important "snapshots"**

28 **reflecting the historical activities of transposons but do not predict current transposition**

29 **potential. We previously reported Sequence-Independent Retrotransposon Trapping (SIRT)**

30 **as a method that, by identification of extrachromosomal linear DNA (eclDNA), revealed**

31 **the presence of active LTR retrotransposons in *Arabidopsis*[3]. However, SIRT cannot be**

32 **applied to large and transposon-rich genomes, as found in crop plants. We have**

33 **developed an alternative approach named ALE-seq (*a*mplification of *L*TR of *e*clDNAs**

34 **followed by *seq*uencing) for such situations. ALE-seq reveals sequences of 5' LTRs of**

35 **eclDNAs after two-step amplification: *in vitro* transcription and subsequent reverse**

36 **transcription. Using ALE-seq in rice, we detected eclDNAs for a novel *Copia* family LTR**

37 **retrotransposon, *Go-on*, which is activated by heat stress. Sequencing of rice accessions**

38 **revealed that *Go-on* has preferentially accumulated in *indica* rice grown at higher**

39 **temperatures. Furthermore, ALE-seq applied to tomato fruits identified a developmentally**

40 **regulated *Gypsy* family of retrotransposons. A bioinformatic pipeline adapted for ALE-seq**

41 **data analyses is used for the direct and reference-free annotation of new, active**

42 **retroelements. This pipeline allows assessment of LTR retrotransposon activities in**

43 **organisms for which genomic sequences and/or reference genomes are either unavailable**

44 **or of low quality.**

45

46 **Main**

47   Chromosomal copies of activated retrotransposons containing long terminal repeats

48 (LTRs) are transcribed by RNA polymerase II, followed by reverse transcription of transcripts

49 to extrachromosomal linear DNAs (eclDNA); these integrate back into host chromosomes[3].

50 Because of the two obligatory template switches during reverse transcription, the newly

51 synthetized eclDNA is flanked by LTRs of identical sequence. Their subsequent divergence

52 due to the accumulation of mutations correlates well with length of time since the last

53 transposition, and thus transposon age[4]. However, the age of LTR retrotransposons cannot

54   be used to predict their current transpositional potential. Moreover, predictions are further

55   complicated by recombination events that occur with high frequency between young and

56   old members of a retrotransposon family[5]; thus old family members also contribute to the

57   formation of novel recombinant elements that insert into new chromosomal positions[5].

58   Although, retrotransposon activities can be relatively easily measured at the transcriptional

59   level[6], the presence of transcripts is a poor predictor of transpositional potential due to

60   posttranscriptional control of this process[7,8]. In addition, direct detection of transposition by

61   genome-wide sequencing to identify new insertions is too expensive and time-consuming to

62   be applied as a screening method. Clearly, the development of an expeditious approach to

63   identify active retrotransposons that predict their transposition potential would be

64   welcomed. We previously described the SIRT strategy for *Arabidopsis* that led to the

65   identification of eclDNA of a novel retroelement and subsequent detection of new

66   insertions[3]. Thus, the presence of eclDNAs, the last pre-integration intermediate, was shown

67   to be a good predictor of retrotransposition potential.

68

69   **Results**

70   <u>Development of ALE-seq</u>

71   Retrotransposons include a conserved sequence known as the primer binding site

72   (PBS), where binding of the 3' end of cognate tRNA initiates the reverse transcription

73   reaction[3]. Met-iCAT (Methionine tRNA-CAT anticodon) PBS was chosen for SIRT as it is the

74   site present in the majority of annotated *Arabidopsis* retrotransposons[3]. To examine

75   whether Met-iCAT PBS sequences are also predominant in LTR retrotransposons of other

76   plants, we used the custom-made software *LTRpred* for *de novo* annotation of LTR

77   retrotransposons in rice and tomato genomes (see Materials and methods). Young

78   retroelements were selected by filtering for at least 95% identity between the two LTRs and

79   subsequently examined for their cognate tRNAs (Supplementary Figure 1). As in *Arabidopsis*,

80   around 80% of LTR retrotransposons in the tomato genome contained Met-iCAT PBS

81   (Supplementary Figure 1). In contrast, only 30% harboured Met-iCAT PBS in rice, and Arg-

82   CCT (Arginine tRNA-CCT anticodon) PBS was found in 60% of young LTR retrotransposons

83   (Supplementary Figure 1). Nonetheless, we used Met-iCAT PBS in our initial experiments

84   because most retrotransposons known to be active in rice callus (e.g. *Tos17* and *Tos19*)

85   contain Met-iCAT PBS. Initially, SIRT was performed on DNA extracted from rice leaves and

86   calli; however, we did not detect eclDNAs for *Tos17* and *Tos19* in rice tissues by this method

87   (Supplementary Figure 2). We reasoned that the short stretch of PBS used for primer design

88   in SIRT may have impaired PCR efficiency due to the many PBS-related sequences present in

89   larger genomes containing a high number of retroelements, as is the case in rice.

90   To counter this problem, we developed an alternative method, named ALE-seq, with

91   significantly improved selectivity and sensitivity of eclDNA detection. A crucial difference to

92   SIRT is that ALE-seq amplification of eclDNA is separated into two reactions: *in vitro*

93   transcription and reverse transcription (Figure 1a). This decoupling of the use of the two

94   priming sequences followed by the digestion of non-templated DNA and RNA is significantly

95   more selective and efficient than the single PCR amplification in SIRT.

96   ALE-seq starts with ligation to the ends of eclDNA of an adapter containing a T7

97   promoter sequence at its 5' end and subsequent *in vitro* transcription with T7 RNA

98   polymerase. The synthesized RNA is then reverse transcribed using the primer that binds

99   the transcripts at the PBS site. The adapter and the oligonucleotides priming reverse

100 transcription are anchored with partial Illumina adapter sequences (Supplementary Table 1),

101 which allows the amplified products to be directly deep-sequenced in a strand-specific

102 manner. The ALE-seq-sequences derived from retrotransposon eclDNAs are predicted to

103 contain the intact 5' LTR up to the PBS site, flanked by Illumina paired-end sequencing

104 adapters. We used the Illumina MiSeq platform for sequencing because its long reads of 300

105 bp from both ends cover the entire LTR lengths of most potentially active elements. It is

106 worth noting that the Illumina adapters were tagged to the intact LTR DNA without

107 fragmentation of the amplicons. This together with the long reads of MiSeq allowed us to

108 reconstitute the complete LTR sequences, even in the absence of the reference genome

109 sequence. The reconstituted LTRs were analysed using the alignment-based approach that

110 complements the mapping-based approach when the reference genome is incomplete

111 (Figure 1b).

112   First, we tested ALE-seq on *Arabidopsis* by examining heat-stressed Col-0

113 *Arabidopsis* plants[9], *met1-1* mutant[3] and epi12[8], a *met1*-derived epigenetic recombinant

4

114   inbred line. ALE-seq cleanly and precisely recovered sequences of complete LTRs for *Onsen*,

115   *Copia21* and *Evade* in samples containing their respective eclDNA (Supplementary Figure

116   3)[3,8,9]. Due to priming of the reverse transcription reaction at PBS, the reads were explicitly

117   mapped to the 5' but not to the 3' LTR, although the two LTRs have identical sequences. The

118   ALE-seq reads have well-defined extremities, starting at the position marking the start of

119   LTRs and finishing at the PBS, which is consistent with their eclDNA origin. The ends of LTRs

120   can also be inspected for conserved sequences that would further confirm their eclDNA

121   origin (Supplementary Figure 4). This reduced ambiguity of read mapping in ALE-seq analysis,

122   combined with the clear-cut detection of LTR ends, allows for explicit and precise

123   assignment of ALE-seq results to active LTR retrotransposons.

124   Since SIRT failed to detect eclDNAs of rice retrotransposons known to be activated in

125   rice callus, we examined whether ALE-seq would identify their eclDNAs. As shown in Figure

126   1c to f, ALE-seq unambiguously detected eclDNAs of *Tos17* and *Tos19* in rice callus, but not

127   in leaf samples. To test whether detection of 5' LTR sequences requires the entire ALE-seq

128   procedure, we performed control experiments with depleted ALE-seq reactions, for example,

129   in the absence of enzymes for either ligation, *in vitro* transcription, or reverse transcription.

130   All incomplete procedures failed to produce sequences containing 5' LTRs derived from

131   eclDNAs (Figure 1e and f). Taken together, the data show that ALE-seq can detect eclDNAs

132   of LTR retrotransposons in *Arabidopsis* as well as in rice with considerably greater efficiency

133   than the SIRT method.

134   To examine the suitability of ALE-seq for quantitative determination of eclDNA levels,

135   we carried out a reconstruction experiment spiking 100 ng of genomic DNA from rice callus

136   with differing amounts of PCR-amplified full-length *Onsen* DNA from 1 ng to 100 fg (Figure

137   2a to d). The results in Figure 2a and b show that the readouts of ALE-seq for *Onsen*

138   correlate well with the input amounts (R^2=0.99). The initial ALE-seq steps of ligation and *in*

139   *vitro* transcription impinged proportionally on the input DNA, resulting in unbiased

140   quantification of the eclDNA and minimal quantitative distortion of the final ALE-seq data.

141   Noticeably, the levels of *Tos17* were similar in all the spiked samples, indicating that

142   addition of *Onsen* DNA did not influence the detection sensitivity of *Tos17*, at least for the

143   amounts tested (Figure 2c and d). Thus, ALE-seq can be used to accurately determine

144   eclDNA levels.

145   Most rice retrotransposons harbour Arg-CCT PBS (Supplementary Figure 1). We

146   tested whether the reverse transcription reaction can be multiplexed to capture both types

147   of retrotransposons (containing Arg-CCT or Met-iCAT PBS) and whether multiplexing of the

148   reverse transcription primers compromises the sensitivity of the procedure. ALE-seq was

149   performed on DNA from rice callus, testing each of the reverse transcription primers

150   separately or as a mixture of both primers in a single reaction. As shown in Figure 2e and

151   Supplementary Figure 5, the levels of *Tos17* recorded in the samples with both primers were

152   similar to the Met-iCAT primer alone. Importantly, we also detected the eclDNAs of the

153   *RIRE2* element containing Arg-CCT PBS (Figure 2f), which was known to be transpositionally

154   active in rice callus[7].

155

156   <u>Identification of *Go-on* retrotransposon using ALE-seq</u>

157   We next used ALE-seq to search for novel active rice retrotransposons. Since many

158   plant retrotransposons are transcriptionally activated by abiotic stresses[9,10], we subjected

159   rice plants to heat stress before subjecting them to ALE-seq. In this way we identified a

160   *Copia*-type retrotransposon able to synthetize eclDNA in the heat-stressed plants (Figure 3a

161   to c) and named this element *Go-on* (the Korean for 'high temperature'). The three

162   retrotransposons with the highest eclDNA levels in heat-stress conditions all belong to the

163   *Go-on* family (Figure 3b and Supplementary Figure 6). Although, eclDNAs were detected for

164   all three copies, *Go-on3* seems to be the youngest and, thus, possibly the most active family

165   member, containing identical LTRs and a complete ORF (Supplementary Figure 6). As

166   depicted in Supplementary Figure 6, the 5' LTR sequences of the three *Go-on* copies are

167   identical; thus the ALE-seq reads derived from *Go-on3* LTR were also cross-mapped to other

168   copies that are possibly inactive or have reduced activities. To further determine whether

169   sequences of *Go-on* LTRs recovered by ALE-seq are indeed derived from *Go-on3* or also from

170   other family members, we performed an ALE-seq experiment using RT primers located

171   further downstream of the PBS, including sequences specific for each *Go-on* family member

172   (Supplementary Figure 6). The amplified ALE-seq products revealed that the eclDNAs

173   produced in heat-stressed rice originated only from *Go-on3* (Supplementary Figure 6). We

174   validated the production of eclDNAs of *Go-on3* by sequencing the junction of the adapter

175   and the 5' end of LTR (Supplementary Figure 6) and by qPCR (Supplementary Figure 7).

176   Next, we examined whether *Go-on3* is transcriptionally activated in rice subjected to

177   heat stress. RNA-seq and the RT-qPCR data clearly showed that *Go-on* is strongly activated

178   in heat-stress conditions (Figure 3d and Supplementary Figure 7). Similar to many other

179   retrotransposons including *ONSEN* of *Arabidopsis*[9,11,12], the LTR sequence of *Go-on3*

180   contains *cis*-acting regulatory element such as the heat shock transcription factor HSFC1-

181   binding sequence motif (Supplementary Figure 7), which is suggestive to its heat stress-

182   mediated transcriptional activation (Figure 3d). To determine whether *Go-on* is also

183   activated in *indica* rice, we heat-stressed plants of *IR64* for three days and examined *Go-on*

184   RNA and DNA levels. Similar to *japonica* rice, *Go-on* RNA and DNA accumulated markedly

185   under heat stress (Supplementary Figure 8), suggesting that the trigger for *Go-on* activation

186   is conserved in both of these evolutionarily distant rice genotypes. Analysis of the RNA-seq

187   data from the heat-stressed rice plants revealed a poor correlation between the mRNA and

188   eclDNA levels of retrotransposons (Supplementary Figure 9). Given that eclDNAs captured

189   by ALE-seq in *Arabidopsis* and rice (Figure 1c to f and Supplementary Figure 3) are all known

190   well for their transposition competence, this possibly agrees with the notion that the

191   eclDNA level is a better predictor of retrotransposition than the RNA level.

192   To possibly relate accumulation of *Go-on* copies in plant populations grown in

193   different temperatures, we analysed the historical retrotransposition of *Go-on* using the

194   genome resequencing data of rice accessions from the 3,000 Rice Genome Project[13]. First,

195   we retrieved the raw sequencing data for all 388 *japonica* rice accessions and the same

196   number of randomly selected sequences of *indica* rice accessions. Using the Transposon

197   Insertion Finder (TIF) tool[14], *japonica* and *indica* sequences were analysed for the number of

198   *Go-on* copies and their genome-wide distribution. Only non-reference insertions that were

199   absent in the reference genome were scored and the cumulative number of new insertions

200   was plotted (Figure 3e to g). Figure 3e shows that the *indica* rice population grown in a

201   warmer climate[15] accumulated significantly more *Go-on* copies than the *japonica* population.

202   As controls, we also examined the accumulation of *Tos17* and *Tos19*, which were not

203   activated by heat stress in our ALE-seq profile (Figure 3a and b). Both retrotransposons

204   showed more transposition events in *japonica* than in *indica* rice (Figure 3f, g and

205   Supplementary Figure 10). Therefore, the copy number of *Go-on* in rice accessions

206   correlated with their growth temperatures, which could possibly be related to occasional

207   *Go-on* activation in elevated ambient temperatures.

208

209   <u>Identification of *FIRE* retrotransposon using ALE-seq</u>

210   It was reported previously that the tomato genome (*Solanum lycopersicum*)

211   experiences a significant loss of DNA methylation in fruits during their maturation, which

212   leads to transcriptional activation of retrotransposons[16]. However, it was not known

213   whether these transcriptionally activated tomato transposons synthesise eclDNA. It was

214   questionable whether the ALE-seq strategy is sensitive enough to detect eclDNA in the ~950

215   Mb tomato genome, which is almost three times as large as ~400 Mb of rice[17]. To address

216   these questions, ALE-seq was carried out on DNA samples from fruits at 52 days post

217   anthesis (DPA), when the loss of DNA methylation is most pronounced[16], and from leaves as

218   a control. It is important to note that we used tomato cultivar (cv.) M82 for these

219   experiments, as it is commonly used for genetic studies[18,19], and that the sequence of the

220   current tomato reference genome is based on cv. Heinz 1706[17]. Since retrotransposon

221   sequences and their chromosomal distributions differ largely between genomes of different

222   varieties within the same plant species[20–22], we could not use the standard mapping-based

223   annotation of the ALE-seq results. As a consequence, we developed a reference-free and

224   alignment-based approach that adopts the clustering of reads based on their sequence

225   similarities (Figure 1b). Briefly, the reads from both samples were pooled and then clustered

226   by sequence homology (See Materials and methods). The consensus of each cluster was

227   determined and used as the reference in paired-end mapping. Subsequently, the consensus

228   sequences were used for a BLAST search against the reference genome for the closest

229   homologues. In this way, the BLAST search was able to map the clustered ALE-seq output to

230   reference genome annotated retrotransposons, which are most similar to the ALE-seq

231   recovered sequences. Applying this strategy, we identified a retroelement belonging to a

232   *Gypsy* family (*FIRE, Fruit-Induced RetroElement*) that produces significant amounts of

233   eclDNA at 52 DPA during fruit ripening (Figure 4a and b). We also determined the transcript

234   levels of the *FIRE* element in leaves and 52 DPA fruit samples. As shown in Figure 4c, fruit

235   RNA levels were enhanced twofold compared to leaves, where *FIRE* eclDNA was barely

236   detectable (Figure 4a). Finally, we found that the DNA methylation status of the *FIRE*

237   element was lower in fruits than leaves in all three sequence contexts (Figure 4d and f). In

238   contrast, the DNA methylation levels of sequences directly flanking *FIRE* were similar in

239   leaves and fruits (Figure 4e to g).

240

241   **Discussion**

242   Recently, a novel active retrotransposon was identified in rice by sequencing

243   extrachromosomal circular DNA (eccDNA) produced as a by-product of retrotransposition or

244   by nuclear recombination reactions of eclDNAs[23,24]. Although the method of eccDNA

245   sequencing has certain advantages over SIRT, such as increased sensitivity and the recovery

246   of sequences of the entire element, it also has certain limitations. For example, the method

247   requires relatively large amounts of starting material but still shows serious limits in

248   efficiency and indicative power for retrotransposition. The method did not detect the

249   eccDNA of *Tos19* in rice callus, where this transposon is known to move[23], however, direct

250   comparison of both methods on the same biological samples was not performed. More

251   importantly, eccDNAs may also be the result of genomic DNA recombination[25] and these

252   background products may be misleading when extrapolating to the transpositional potential

253   of a previously unknown element. In this respect, ALE-seq is a significantly improved tool

254   that largely overcomes the above-mentioned limitations of previous methods and requires

255   only 100 ng of plant DNA.

256   The heat-responsiveness of *Go-on*, the novel heat-activated *Copia* family

257   retrotransposon of rice detected using ALE-seq, seems to be conferred by *cis*-acting DNA

258   elements embedded in the LTR, which are similar to the heat-activated *Onsen*

259   retrotransposon in *Arabidopsis*[11,12]. Although heat stress can induce production of mRNA

260   and eclDNA of *Onsen*, its retrotransposition is tightly controlled by the small interfering RNA

261   pathway[9]. Given that real-time transposition of rice retrotransposons has only been

262   detected in epigenetic mutants[26,27] and triggered by tissue culture conditions causing vast

263   alterations in the epigenome[7],or as a result of interspecific hybridization[28], an altered

264   epigenomic status seems to be an important prerequisite for retrotransposition. In fact, we

265   failed to detect transposed copies of *Go-on* in the progeny of heat-stressed rice plants. Thus,

266   although *Go-on* produces eclDNAs after heat stress, it may be mobilized only at low

267   frequency in wild type rice due to epigenetic restriction of retrotransposition. Nevertheless,

268   on an evolutionary scale, the higher number of new insertions of *Go-on* in *indica* rice

269   populations grown at elevated temperatures might suggest its potential mobility.

270   Many retrotransposons are transcriptionally reactivated during specific

271   developmental stages or in particular cell types[29,30]. In tomato, fruit pericarp exhibits a

272   reduction in DNA methylation during ripening[16]. This is largely attributed to higher

273   transcription of the *DEMETER-LIKE2* DNA glycosylase gene[31]. Despite massive transcriptional

274   reactivation of retrotransposons in tomato fruits, it has been difficult to determine whether

275   further steps toward transposition also take place. Using ALE-seq, we identified eclDNA that

276   we annotated using a reference-free and alignment-based approach to a novel *FIRE* element.

277   *FIRE* has 164 copies in the reference tomato genome and in a conventional mapping-based

278   approach the ALE-seq reads of *FIRE* cross-mapped to multiple copies, making it difficult to

279   assign eclDNA levels to particular family members (Supplementary Figure 11). Therefore,

280   our strategy can be used in situations where sequence of the reference genome is

281   unavailable or the mapping of reads is hindered by the high complexity and multiplicity of

282   the retrotransposon population.

283   ALE-seq could also be applied to non-plant systems. For example, numerous studies

284   in various eukaryotes, including mammals, found that retrotransposons are transcriptionally

285   activated by certain diseases or at particular stages during embryo development[32,33]. It was

286   also suggested that retrotransposition might be an important component of disease

287   progression[34]. Given that the direct detection of retrotransposition is challenging, it would

288   be interesting to use ALE-seq to determine whether such temporal relaxations of epigenetic

289   transposon silencing also result in the production of the eclDNAs, as the direct precursor of

290   the chromosomal integration of a retrotransposon.

291

292

Materials and methods

Plant materials

Seeds of *Oryza sativa ssp. japonica cv. Nipponbare* and *Oryza sativa ssp. indica cv. IR64* were surface-sterilized in 20% bleach for 15 min, rinsed three times with sterile water and germinated on ½-MS media. Rice plants were grown in 10 h light / 14 h dark at 28°C and 26°C, respectively. For heat-stress experiments, 1-week-old rice plants were transferred to a growth chamber at 44°C and 28°C in light and dark, respectively. Rice callus was induced by the method used for rice transformation as previously described[35].

Tomato plants (*Solanum lycopersicum cv. M82*) were grown under standard greenhouse conditions (16 h supplemental lighting of 88 w/m^2 at 25°C and 8 h at 15°C). Tomato leaf tissue samples were taken from 2-month-old plants. Tomato fruit pericarp tissues were harvested at 52 days post anthesis (DPA).

Annotation of LTR retrotransposons

Functional *de novo* annotation of LTR retrotransposons for the genomes of TAIR10 (Arabidopsis), MSU7 (rice) and SL2.50 (tomato) was achieved by the *LTRpred* pipeline (https://github.com/HajkD/LTRpred) using the parameter configuration: minlenltr = 100, maxlenltr = 5000, mindistltr = 4000, maxdisltr = 30000, mintsd = 3, maxtsd = 20, vic = 80, overlaps = "no", xdrop = 7, motifmis = 1 , pbsradius = 60, pbsalilen = c(8,40), pbsoffset = c(0,10), quality.filter = TRUE, n.orf = 0. The plant-specific tRNAs used to screen for primer binding sites (PBS) were retrieved from GtRNAdb[36] and plantRNA[37] and combined in a custom fasta file. The hidden Markov model files for gag and pol protein conservation screening were retrieved from Pfam[38] using the protein domains RdRP_1 (PF00680), RdRP_2 (PF00978), RdRP_3 (PF00998), RdRP_4 (PF02123), RVT_1 (PF00078), RVT_2 (PF07727), Integrase DNA binding domain (PF00552), Integrase zinc binding domain (PF02022), Retrotrans_gag (PF03732), RNase H (PF00075) and Integrase core domain (PF00665). Computationally reproducible scripts for generating annotations can be found at http://github.com/HajkD/ALE.

321

<u>ALE-seq library preparation</u>

Genomic DNA was extracted using a DNeasy Plant Mini Kit (Qiagen) following the manufacturer's instruction. Genomic DNA (100 ng) was used for adapter ligation with 4 µl of 50 µM adapter DNA. After an overnight ligation reaction at 4°C, the adapter-ligated DNA was purified by AMPure XP beads (Beckman Coulter) at a 1:0.5 ratio. *In vitro* transcription reactions were performed using a MEGAscript RNAi kit (Thermo Fisher) with minor modifications. Briefly, the reaction was carried out for 4 h at 37°C and the template DNA was digested prior to RNA purification. Purified RNA (3 µg) was subjected to reverse transcription (RT) using a Transcriptor First Strand cDNA Synthesis Kit (Roche). Transcriptor First Strand cDNA Synthesis Kit was chosen because the RTase of the kit is thermostable. This allowed the RT reaction at higher temperature (55°C) that reduces the RT-inhibiting RNA secondary structure formation. The custom RT primers were added as indicated for each experiment. After the RT reaction, 1 µl of RNase A/T1 (Thermo Fisher) was added to digest non-templated RNA and the reaction mixture was incubated at 37°C for at least 30 min. Single-stranded first strand cDNA was PCR-amplified by 25 cycles using Illumina TruSeq HT dual adapter primers and the PCR product was purified by AMPure XP beads (Beckman Coulter) at a 1:1 ratio. After purification, the eluted DNA was quantified using a KAPA Library Quantification Kit (KAPA Biosystems) and run on the MiSeq v3 2 X 300 bp platform in the Department of Pathology of the University of Cambridge. Due to the nature of ALE-seq that specifically amplifies ecDNAs, some ecDNA-free samples did not produce enough library DNAs which, although suboptimal loading, were nevertheless sequenced. It is advisable to spike in PCR-amplified retrotransposon DNA as described below. The oligonucleotide sequences are provided in Supplementary Table 1.

<u>Preparation of full-length *Onsen* DNA</u>

The full-length *Onsen* copy (AT1TE12295) was amplified using Phusion High-Fidelity DNA polymerase (New England Biolabs). PCR products were run on 1% agarose gels. The full-length fragment was then purified by QIAquick Gel Extraction (Qiagen) and its concentration

350   was measured using the Qubit Fluorometric Quantitation system (Thermo Fisher). Primers

351   used for amplification are listed in Supplementary Table 1.

352

353   RT-qPCR analyses

354   Samples were ground in liquid nitrogen using mortar and pestle. An RNeasy Plant Mini Kit

355   (Qiagen) was used to extract total RNA following the manufacturer's instructions. The

356   amount of extracted RNA was estimated using the Qubit Fluorometric Quantitation system

357   (Thermo Fisher). cDNAs were synthesized using a SuperScript VILO cDNA Synthesis Kit

358   (Invitrogen). Real-time quantitative PCR was performed in the LightCycler 480 system

359   (Roche) using primers listed in Supplementary Table 1. LightCycler 480 SYBR green I master

360   premix (Roche) was used to prepare the reaction mixture in a volume of 10 µl. The results

361   were analysed by the ΔΔCt method.

362

363   RNA-seq library construction

364   Total RNA was prepared as described above. An Illumina TruSeq Stranded mRNA Library

365   Prep kit (Illumina) was used according to the manufacturer's instructions. The resulting

366   library was run on an Illumina NextSeq 500 machine (Illumina) in the Sainsbury Laboratory

367   at the University of Cambridge.

368

369   Analysis of next-generation sequencing data

370   For RNA-seq data analysis, the adapter and the low-quality sequences were removed by

371   Trimmomatic software[39]. The cleaned reads were mapped to the MSU7 version of the rice

372   reference genome (http://rice.plantbiology.msu.edu) using TopHat2[40]. The resulting

373   mapping files were processed to the Cufflinks/Cuffquant/Cuffnorm pipeline[41] guided by the

374   annotation file which includes the MSU7 reference gene annotation

375   (http://rice.plantbiology.msu.edu/pub/data/Eukaryotic_Projects/o_sativa/annotation_dbs/

376   pseudomolecules/version_7.0/all.dir/) and our custom retrotransposon annotation.

377 Visualization of sequencing data was performed using an Integrative Genomics Viewer

378 (IGV)[42].

379 For ALE-seq data analysis, the adapter sequence was removed from the raw reads using

380 Trimmomatic software. For the mapping-based approach, paired-end reads were mapped to

381 the reference genomes (Arabidopsis, TAIR10; rice, MSU7; tomato, SL2.50) using Bowtie2[43]

382 with minor optimization. In most short-read sequencing platforms, it is often difficult to

383 assign the multi-mapped reads of TEs to precise genomic location. However, as MiSeq

384 outputs relatively longer reads, we presumed that ALE-seq reads have less ambiguity than

385 other sequencing platforms and set the parameters dealing with multi-mappers to default.

386 It is only the maximum fragment length option which is set to 500 by default that was

387 manipulated to 3000 (-X 3000). The numbers of reads mapped throughout each

388 retrotransposon were counted by the featureCounts tool of the SubRead package[44] using

389 the custom annotation file created by *LTRpred*. Since featureCounts recognizes multi-

390 mappers by SAM file's NH tag that bowtie2 does not generate, multi-mapped reads are

391 counted as one read aligned to a single genomic location, which reduces quantitation bias

392 that often happens to multi-mappers. IGV was used to visualize the sequencing data. For the

393 alignment-based approach, the forward and reverse reads were merged to yield the full-

394 length fragment sequences and converted to fasta files using the BBTools

395 (https://jgi.doe.gov/data-and-tools/bbtools/). The fasta files created for all the samples

396 were concatenated to get a master fasta file that is later inputted to CD-HIT software[45] to

397 cluster the reads by sequence similarity with the following options: -c 0.95, -ap 1, -g 1. CD-

398 HIT outputs a fasta file of representative reads for each cluster. The resulting fasta file was

399 used as reference for paired-end mapping of initial fastq files. The mapped reads were

400 counted with the featureCounts tool. Those clusters that significantly differed in the number

401 of mapped reads in different samples were further analysed for their identities using BLAST

402 search.

403 For Bisulfite sequencing analysis, raw sequenced reads derived from tomato fruits (52 DPA)

404 and leaves were downloaded from the public repository (SRP008329)[16] and re-analysed as

405 previously described[46], with minor modifications. Briefly, high-quality sequenced reads were

406 mapped with Bismark[47] on the cv. Heinz 1706 reference genome (https://solgenomics.net),

407 including a chloroplast sequence obtained from GenBank database (NC_007898.3) to

14

408   estimate the conversion rate. After methylation call and correction for unconverted

409   cytosines, the methylation proportions at each cytosine position with a coverage of at least

410   3 reads were used to generate a bedGraph file for each cytosine context, using the R

411   Bioconductor packages DMRCaller[48] and Rtracklayer[49]. The IGV browser was used to

412   visualize the methylation profiles.

413

414   <u>Detection of retrotransposon insertions</u>

415   The insertions of selected retrotransposons were detected from the genome resequencing

416   data of *japonica* and *indica* rice accessions downloaded from the 3,000 rice genome project

417   (PRJEB6180). The Transposon Insertion Finder (TIF) program[14] was used to identify the split

418   reads in the fastq files and detect newly integrated copies. We used MSU7

419   (http://rice.plantbiology.msu.edu) and ShuHui498 (http://www.mbkbase.org) for the

420   reference of *japonica* and *indica* rice, respectively. Only non-reference insertions were

421   considered and common insertions found in multiple accessions were counted as a single

422   retrotransposition event.

423

424   <u>Data availability</u>

425   The next generation sequencing data that support the findings of this study are available in

426   the Sequence Read Archive (SRA) repository with the identifier SRP155920.

427

428   <u>Code availability</u>

429   The custom scripts used in this study are available in http://github.com/HajkD/ALE.

430

References

431

432   1.   Lisch, D. How important are transposons for plant evolution? *Nat Rev Genet* **14,** 49–

433   61 (2012).

434   2.   Chuong, E. B., Elde, N. C. & Feschotte, C. Regulatory activities of transposable

435   elements: from conflicts to benefits. *Nat. Rev. Genet.* **18,** 71–86 (2017).

436   3.   Griffiths, J., Catoni, M., Iwasaki, M. & Paszkowski, J. Sequence-Independent

437   Identification of Active LTR Retrotransposons in Arabidopsis. *Mol. Plant* **11,** 508–511

438   (2017).

439   4.   Ma, J. & Bennetzen, J. L. Rapid recent growth and divergence of rice nuclear genomes.

440   *Proc. Natl. Acad. Sci. U. S. A.* **101,** 12404–12410 (2004).

441   5.   Sanchez, D. H., Gaubert, H., Drost, H., Zabet, N. R. & Paszkowski, J. High-frequency

442   recombination between members of an LTR retrotransposon family during

443   transposition bursts. *Nat. Commun.* **8,** 1–6 (2017).

444   6.   Picault, N. *et al.* Identification of an active LTR retrotransposon in rice. *Plant J.* **58,**

445   754–765 (2009).

446   7.   Sabot, F. *et al.* Transpositional landscape of the rice genome revealed by paired-end

447   mapping of high-throughput re-sequencing data. *Plant J.* **66,** 241–246 (2011).

448   8.   Mirouze, M. *et al.* Selective epigenetic control of retrotransposition in Arabidopsis.

449   *Nature* **461,** 427–430 (2009).

450   9.   Ito, H. *et al.* An siRNA pathway prevents transgenerational retrotransposition in

451   plants subjected to stress. *Nature* **472,** 115–119 (2011).

452   10.   Paszkowski, J. Controlled activation of retrotransposition for plant breeding. *Curr.*

453   *Opin. Biotechnol.* **32,** 200–206 (2015).

454   11.   Cavrak, V. V. *et al.* How a Retrotransposon Exploits the Plant's Heat Stress Response

455   for Its Activation. *PLoS Genet.* **10,** 1–12 (2014).

456   12.   Pietzenuk, B. *et al.* Recurrent evolution of heat-responsiveness in Brassicaceae COPIA

457   elements. *Genome Biol.* 1–15 (2016). doi:10.1186/s13059-016-1072-3

458   13.   The 3, 000 rice genomes project. The 3 , 000 rice genomes project. *Gigascience* **3,** 1–6
459   (2014).

460   14.   Nakagome, M. *et al.* Transposon Insertion Finder (TIF): a novel program for detection
461   of de novo transpositions of transposable elements. *BMC Bioinformatics* **15,** 1–9
462   (2014).

463   15.   Xiong, Z. Y. *et al.* Latitudinal Distribution and Differentiation of Rice Germplasm : Its
464   Implications in Breeding. *Crop Sci.* **51,** 1050–1058 (2011).

465   16.   Zhong, S. *et al.* Single-base resolution methylomes of tomato fruit development
466   reveal epigenome modifications associated with ripening. *Nat. Biotechnol.* **31,** 154–
467   159 (2013).

468   17.   Consortium, T. tomato genome. The tomato genome sequence provides insights into
469   fleshy fruit evolution. *Nature* **485,** 635–641 (2012).

470   18.   Eshed, Y. & Zamir, D. An Introgression Line Population of Lycopersicon pennellii in the
471   Cultivated Tomato Enables the Identification and Fine Mapping of Yield-Associated
472   QTL. *Genetics* **141,** 1147–1162 (1995).

473   19.   Eshed, Y. & Zamir, D. Less-Than-Additive Epistatic Interactions of Quantitative Trait
474   Loci in Tomato. *Genetics* **143,** 1807–1817 (1996).

475   20.   Quadrana, L. *et al.* The Arabidopsis thaliana mobilome and its impact at the species
476   level. *Elife* **5,** 1–25 (2016).

477   21.   Stuart, T. *et al.* Population scale mapping of transposable element diversity reveals
478   links to gene regulation and epigenomic variation. *Elife* **5,** 1–27 (2016).

479   22.   Wei, B. *et al.* Genome-wide characterization of non-reference transposons in crops
480   suggests non-random insertion. *BMC Genomics* **17,** 1–13 (2016).

481   23.   Lanciano, S. *et al. Sequencing the extrachromosomal circular mobilome reveals*
482   *retrotransposon activity in plants*. *PLOS Genetics* **13,** (2017).

483   24.   Møller, H. D. *et al.* Formation of Extrachromosomal Circular DNA from Long Terminal
484   Repeats of Retrotransposons in Saccharomyces cerevisiae. *G3 (Bethesda).* **6,** 453–462
485   (2015).

486   25.   Møller, H. D., Parsons, L., Jørgensen, T. S., Botstein, D. & Regenberg, B.
487   Extrachromosomal circular DNA is common in yeast. *Proc. Natl. Acad. Sci. U. S. A.* **112,**
488   3114–3122 (2015).

489   26.   Cheng, C. *et al.* Loss of function mutations in the rice chromomethylase OsCMT3a
490   cause a burst of transposition. *Plant J.* **83,** 1069–1081 (2015).

491   27.   Cui, X. *et al* Control of transposon activity by a histone H3K4 demethylase in rice.
492   *Proc. Natl. Acad. Sci. U. S. A.* **110,** 1953–1958 (2013).

493   28.   Wang, Z. H. *et al.* Genomewide Variation in an Introgression Line of Rice-Zizania
494   Revealed by Whole-Genome re-Sequencing. *PLoS One* **8,** 1–12 (2013).

495   29.   Li, H., Freeling, M. & Lisch, D. Epigenetic reprogramming during vegetative phase
496   change in maize. *Proc. Natl. Acad. Sci. U. S. A.* **107,** 22184–22189 (2010).

497   30.   Slotkin, R. K. *et al.* Epigenetic Reprogramming and Small RNA Silencing of
498   Transposable Elements in Pollen. *Cell* **136,** 461–472 (2009).

499   31.   Liu, R. *et al* A DEMETER-like DNA demethylase governs tomato fruit ripening. *Proc.*
500   *Natl. Acad. Sci.* **112,** 10804–10809 (2015).

501   32.   Goodier, J. L. Retrotransposition in tumors and brains. *Mobile DNA* **5,** 1–6 (2014).

502   33.   Baillie, J. K. *et al.* Somatic retrotransposition alters the genetic landscape of the
503   human brain. *Nature* **479,** 534–537 (2011).

504   34.   Mullins, C. S. & Linnebacher, M. Human endogenous retroviruses and cancer :
505   Causality and therapeutic possibilities. *World J. Gastroenterol.* **18,** 6027–6035 (2012).

506   35.   Cho, J. & Paszkowski, J. Regulation of rice root development by a retrotransposon
507   acting as a microRNA sponge. *Elife* **6,** 1–21 (2017).

508   36.   Chan, P. P. & Lowe, T. M. GtRNAdb 2 . 0 : an expanded database of transfer RNA

509   genes identified in complete and draft genomes. *Nucleic Acids Res.* **44,** 184–189

510   (2016).

511   37.   Daujat, M. *et al.* PlantRNA , a database for tRNAs of photosynthetic eukaryotes.

512   *Nucleic Acids Res.* **41,** 273–279 (2012).

513   38.   Finn, R. D. *et al.* Pfam : the protein families database. *Nucleic Acids Res.* **42,** 222–230

514   (2014).

515   39.   Bolger, A. M., Lohse, M. & Usadel, B. Trimmomatic : a flexible trimmer for Illumina

516   sequence data. *Bioinformatics* **30,** 2114–2120 (2014).

517   40.   Kim, D. *et al.* TopHat2 : accurate alignment of transcriptomes in the presence of

518   insertions , deletions and gene fusions. *Genome Biol.* **14,** 1–13 (2013).

519   41.   Trapnell, C. *et al.* Transcript assembly and quantification by RNA-Seq reveals

520   unannotated transcripts and isoform switching during cell differentiation. *Nat.*

521   *Biotechnol.* **28,** 516–520 (2010).

522   42.   Robinson, J. T. *et al.* Integrative Genomics Viewer. *Nat. Biotechnol.* **29,** 24–26 (2011).

523   43.   Langmead, B. & Salzberg, S. L. Fast gapped-read alignment with Bowtie 2. *Nat.*

524   *Methods* **9,** 357–359 (2013).

525   44.   Liao, Y., Smyth, G. K. & Shi, W. The Subread aligner : fast , accurate and scalable read

526   mapping by seed-and-vote. *Nucleic Acids Res.* **41,** 1–17 (2013).

527   45.   Li, W. & Godzik, A. Cd-hit : a fast program for clustering and comparing large sets of

528   protein or nucleotide sequences. *Bioinformatics* **22,** 1658–1659 (2006).

529   46.   Catoni, M. *et al.* DNA sequence properties that predict susceptibility to epiallelic

530   switching. *EMBO* **36,** 617–628 (2017).

531   47.   Krueger, F. & Andrews, S. R. Bismark : a flexible aligner and methylation caller for

532   Bisulfite-Seq applications. *Bioinformatics* **27,** 1571–1572 (2011).

533   48.   Catoni, M., Tsang, J. M. F., Greco, A. P. & Zabet, N. R. DMRcaller : a versatile R /

534   Bioconductor package for detection and visualization of differentially methylated

535   regions in CpG and non-CpG contexts. *Nucleic Acids Res.* 1–11 (2018).

536 49. Lawrence, M., Gentleman, R. & Carey, V. rtracklayer : an R package for interfacing

537   with genome browsers. *Bioinformatics* **25,** 1841–1842 (2009).

538

Author Contributions

J.C. and J.P. conceived the research. J.C., M.B., M.C., H.-G.D., A.B. and M.O. performed experiment. J.C., M.B., M.C. and H.-G.D. analysed data. J.C. and J.P. wrote and revised the manuscript.

Competing Interests

The authors declare that no competing interests exist.

Corresponding authors

Correspondence to Jungnam Cho (jungnam.cho@slcu.cam.ac.uk) and Jerzy Paszkowski (jerzy.paszkowski@slcu.cam.ac.uk).

Figure Legends

Figure 1. Detection of eclDNA by ALE-seq

a, The workflow of ALE-seq. The colour code is indicated in a box. **b**, Analysis pipeline of ALE-
seq results. The sequenced reads can be mapped to the reference genome or aligned to
each other to obtain a cluster consensus. **c** and **d**, Genome-wide plots of rice ALE-seq results
from leaf (**c**) and callus (**d**). The levels are shown as number of reads mapped to each
retrotransposon. Dots represent annotated retrotransposons; those corresponding to *Tos17*
and *Tos19* are indicated. **e** and **f**, Read coverage plots mapped to *Tos17* (**e**) and *Tos19* (**f**).
The black bars represent retrotransposons and white arrowheads indicate LTRs.

Figure 2. Sensitivity and specificity of eclDNA detection by ALE-seq

a-**d**, ALE-seq reconstruction experiment with varying amounts of PCR-amplified *Onsen* DNA
added to rice callus DNA. Genome browser image with the read coverage (**a** and **c**) and
quantitated read counts (**b** and **d**) for *Onsen* (**a** and **b**) and *Tos17* (**c** and **d**) loci. The amounts
of *Onsen* DNA added were 1 ng, 100 pg, 10 pg, 1 pg or 100 fg; 100 ng of rice callus DNA was
used. Note that read coverage values are $\log_{10}$-converted in **a**. For **b** and **d**, values are shown
as $\log_{10}$-converted counts per million sequenced reads. **e** and **f**, Read coverage plots for the
ALE-seq of rice callus using different RT primers. *Tos17* and *RIRE2* transposons are depicted
below the plots as in Figure 1.

Figure 3. Identification of a novel heat-activated retrotransposon in rice

a and **b**, Genome-wide plots of rice ALE-seq results as in Figure 1. Control (**a**) and heat-
stressed (**b**) rice plants were used. One-week-old seedlings were subjected to heat stress
(44°C) for 3 days. Met-iCAT PBS primer was used in RT. The levels are shown as the number
of reads mapped to retroelements. Three *Go-on* copies are indicated in **b**. **c**, Read coverage
plot for *Go-on3*. **d**, RNA-seq data showing *Go-on3* and a neighbouring gene. RNA-seq data
were generated using the same plant materials as in **a** and **b**. The experiment was repeated
independently two times with similar results. **e**-**g**, Cumulative plots for the number of non-

584 reference insertions of *Go-on* (**e**), *Tos17* (**f**), and *Tos19* (**g**) in the genomes of 388 *japonica*

585 and *indica* rice accessions. The statistical difference was determined by iterating random

586 selection of 200 accessions out of 388 and performing the two-tailed Wilcoxon test. ** *P*
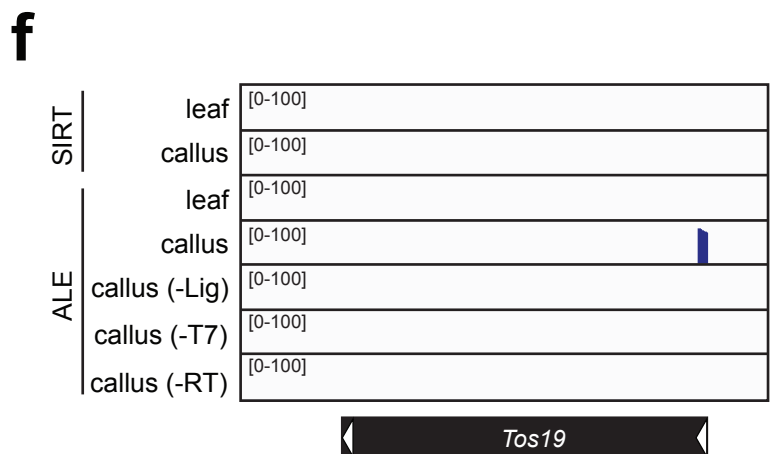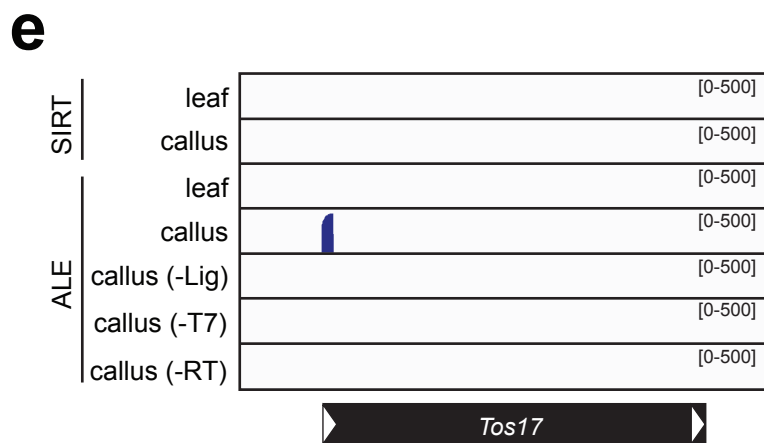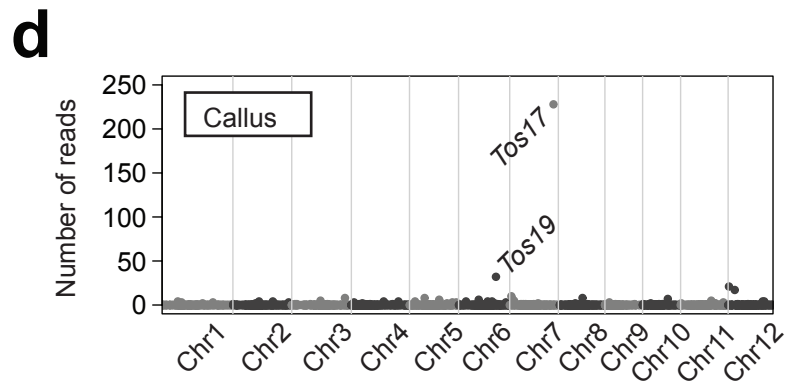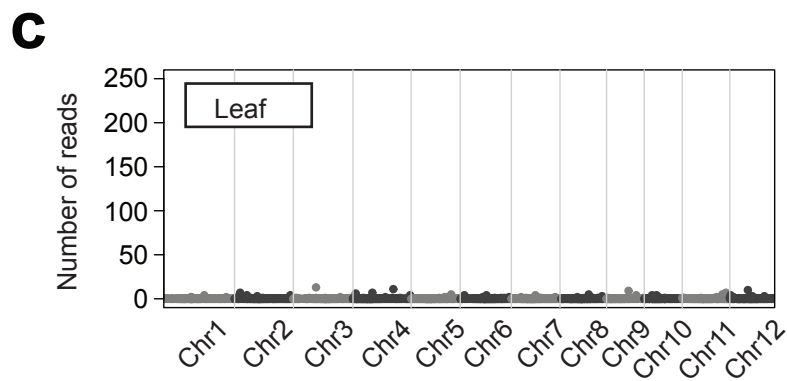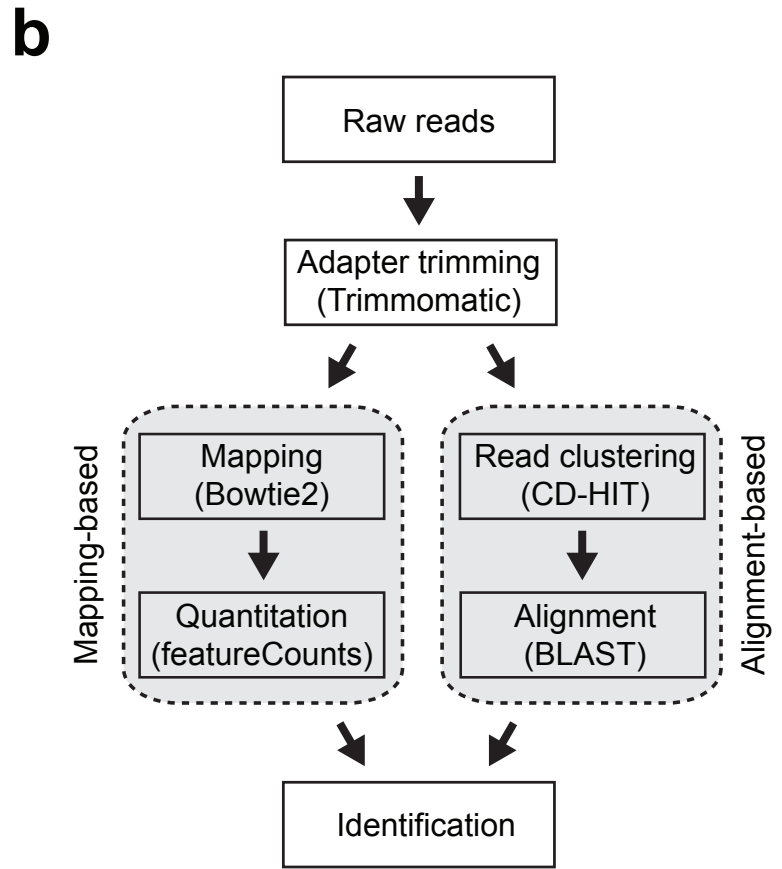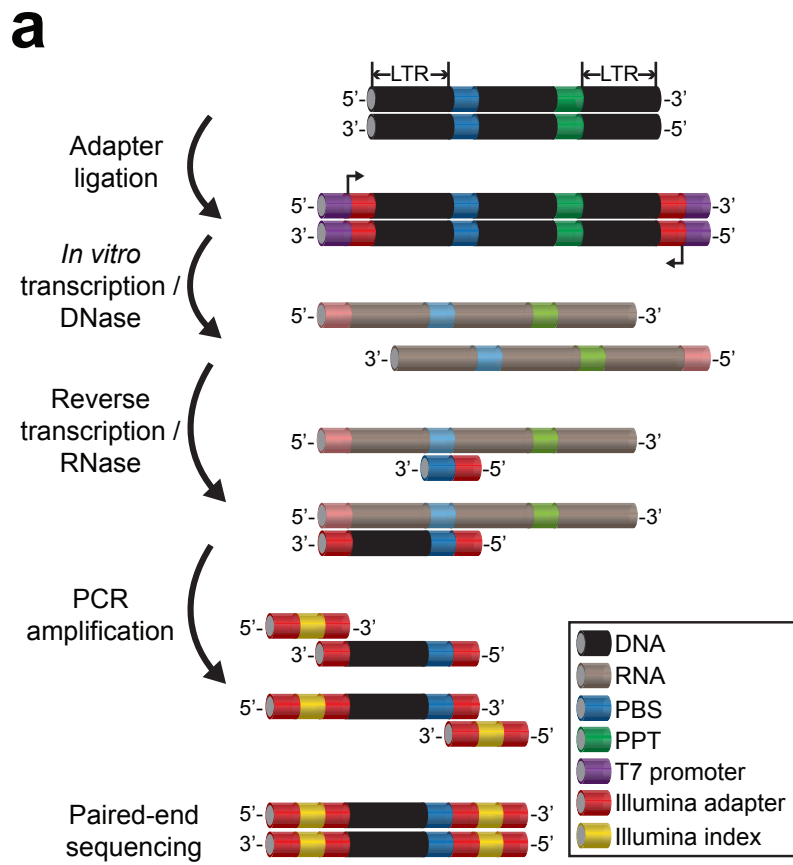
587 $=2.2e^{-16}$.

588

589 Figure 4. Identification of a tomato retrotransposon activated in fruit pericarp

590 **a**, Read coverage plot for the *FIRE* retrotransposon identified in tomato fruit pericarp by

591 ALE-seq. Met-iCAT PBS primer was used in RT. **b** and **c**, The DNA (**b**) and RNA (**c**) levels of

592 *FIRE* in leaves and fruits determined by qPCR. The levels are means of two biological

593 replicates. Normalization was done against *SlGAPDH* (Solyc03g111010) and *SlCAC*

594 (Solyc08g006960) for DNA and RNA analyses, respectively. **d**, Genome browser image for

595 the DNA methylation levels at *FIRE* element in leaves and fruits of tomato. The levels are

596 shown as percent methylation of each cytosine. **e**-**g**, Violin plots for DNA methylation levels

597 at the upstream (**e**), *FIRE* (**f**) and downstream (**g**) regions. Only cytosines supported by at

598 least three reads in both samples were considered. In *FIRE* locus, for example, 4,032 out of

599 4,078 cytosines in both strands were analysed. The upstream and downstream regions are

600 immediate flanking sequences taken for the same length as *FIRE* of 9.362 kb. P-values were

601 determined by a two-sided Fisher's t-test using 558 CG and 717 CHG sites at *FIRE* locus.

602 Other samples with insignificant statistical difference are not shown for the p-values.
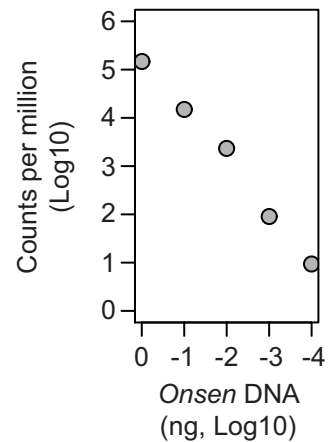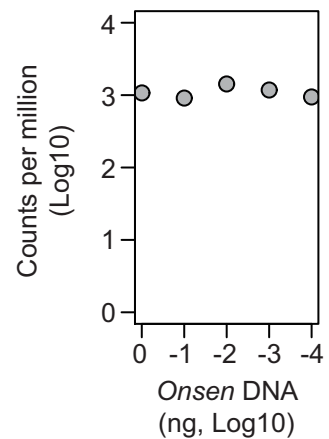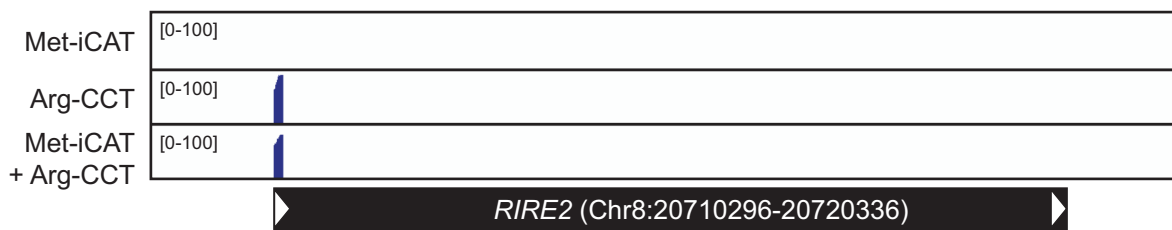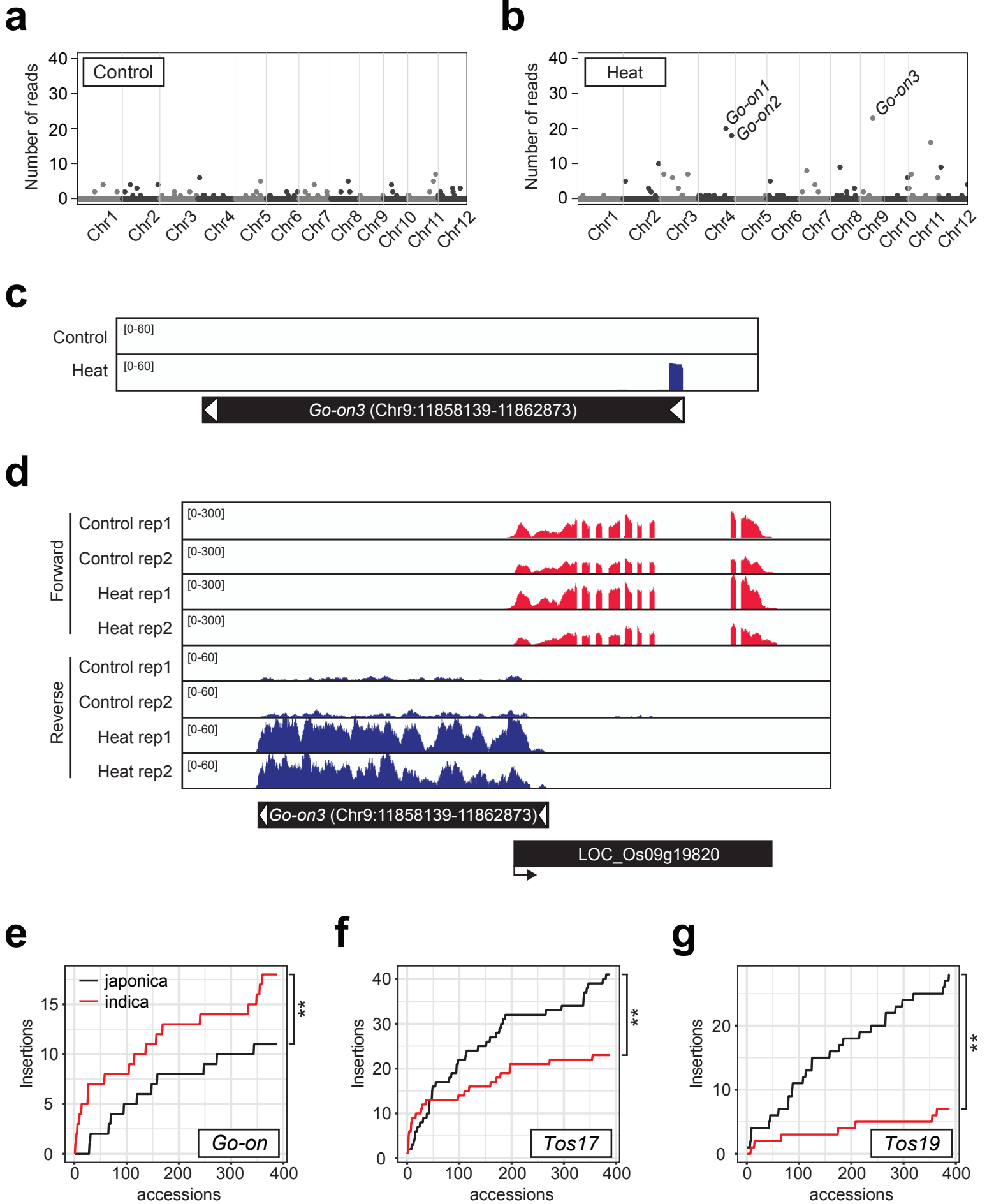
603

Figure 1.

Figure 2.

a

[0-7]
[0-7]
[0-7]
[0-7]
[0-7]

Onsen DNA

Onsen (AT1TE12295)

b

Counts per million (Log10)

Onsen DNA
(ng, Log10)

c

[0-500]
[0-500]
[0-500]
[0-500]
[0-500]

Onsen DNA

Tos17 (Chr7:26694787-26698920)

d

Counts per million (Log10)

Onsen DNA
(ng, Log10)

e

Met-iCAT [0-500]
Arg-CCT [0-500]
Met-iCAT
+ Arg-CCT [0-500]

Tos17 (Chr7:26694787-26698920)

f

Met-iCAT [0-100]
Arg-CCT [0-100]
Met-iCAT
+ Arg-CCT [0-100]

RIRE2 (Chr8:20710296-20720336)

Figure 3.

a

b

c

d

e

f

g
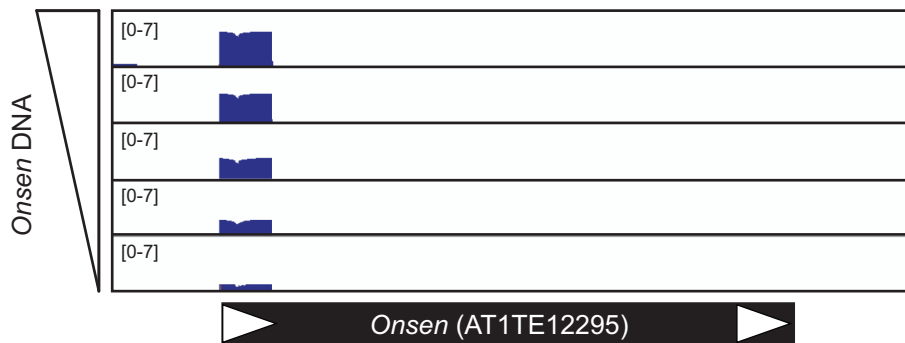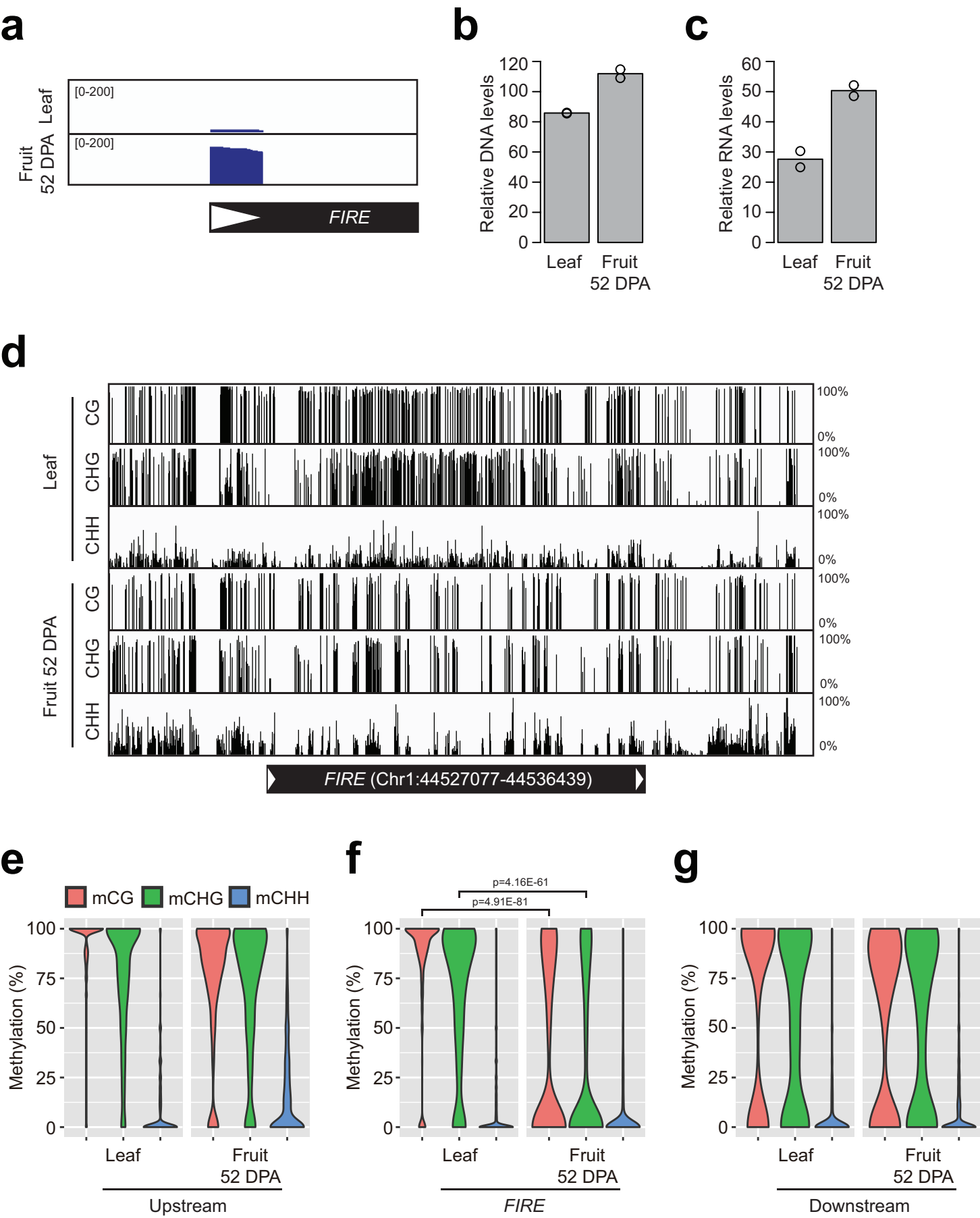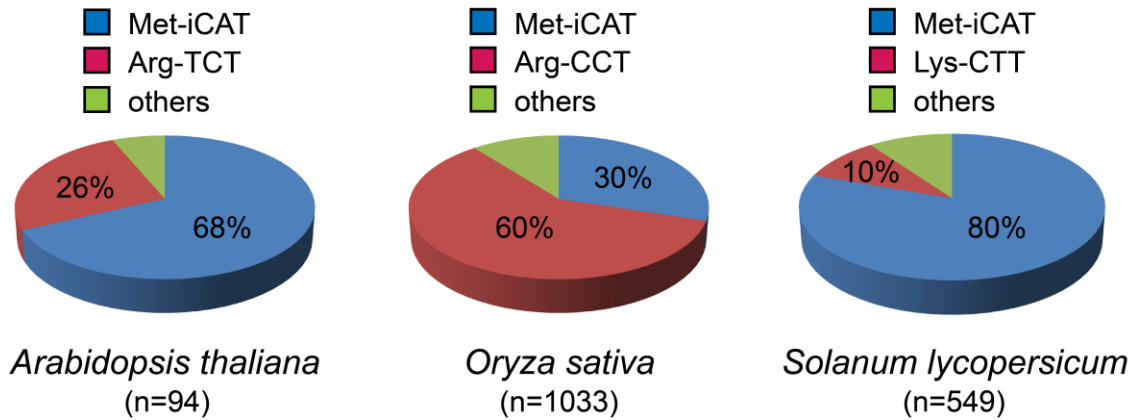
Figure 4.

Supplementary Figure 1. PBS sequences of LTR retrotransposons in *Arabidopsis*, rice and tomato

The frequency of tRNAs used for targeting PBS. LTR retrotransposons were annotated by *LTRpred* (http://github.com/HajkD/ALE) and selected for young elements by filtering LTR similarities higher than 95%. The total numbers of retrotransposons analysed in each species are shown below the plots.
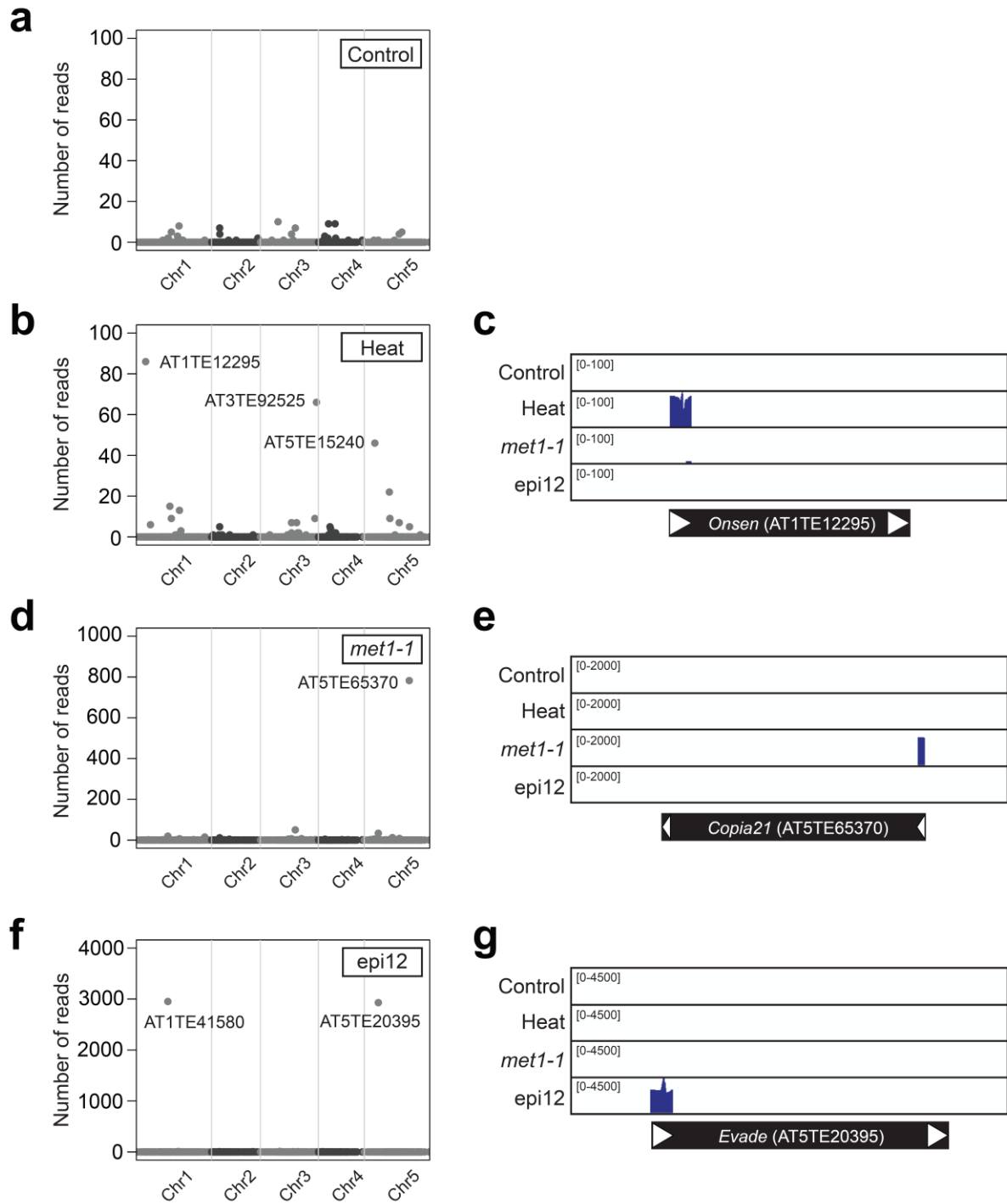
a
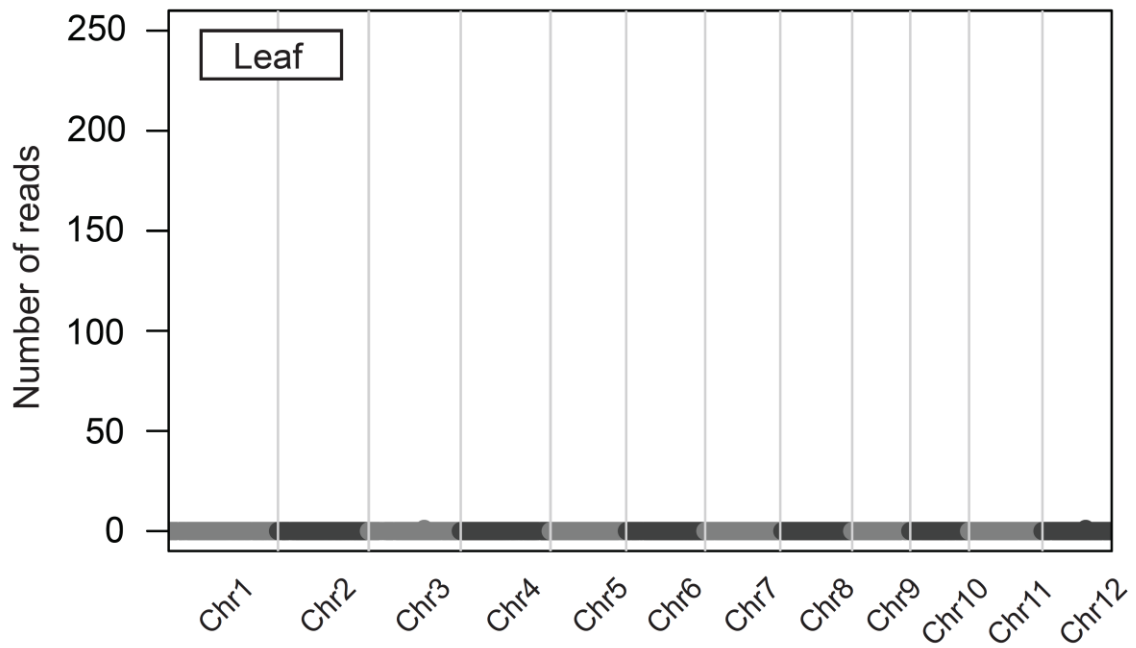
b
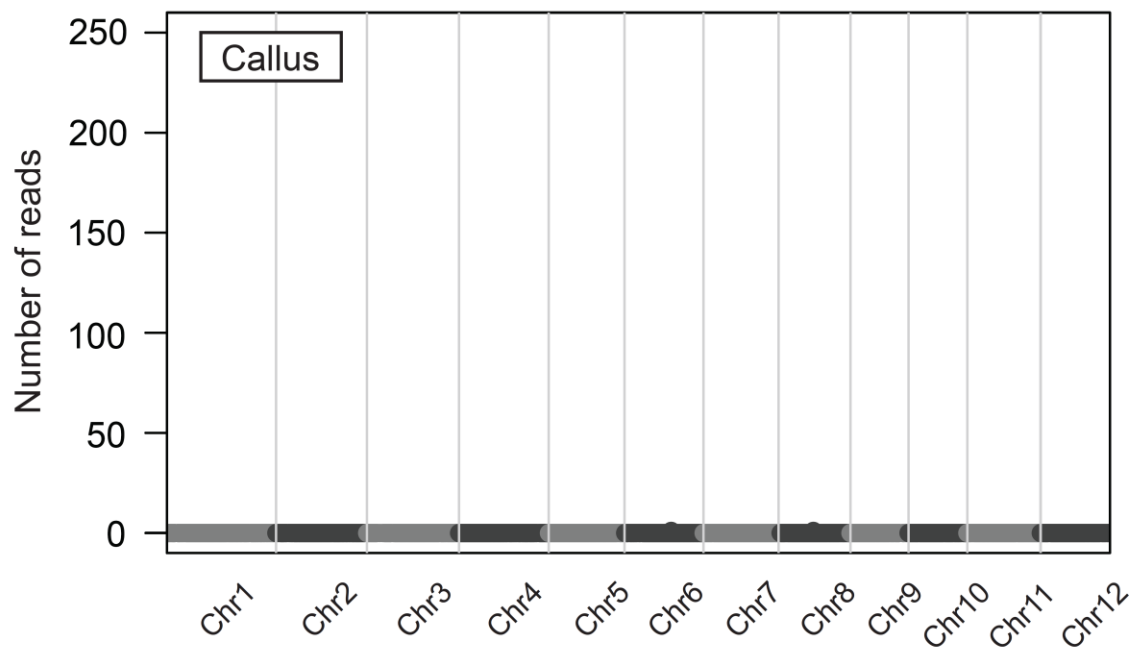
9

10   **Supplementary Figure 2.** SIRT results from leaves and calli of rice

11   **a** and **b,** Genome-wide plots for SIRT performed in leaves (**a**) and in calli (**b**) of rice.
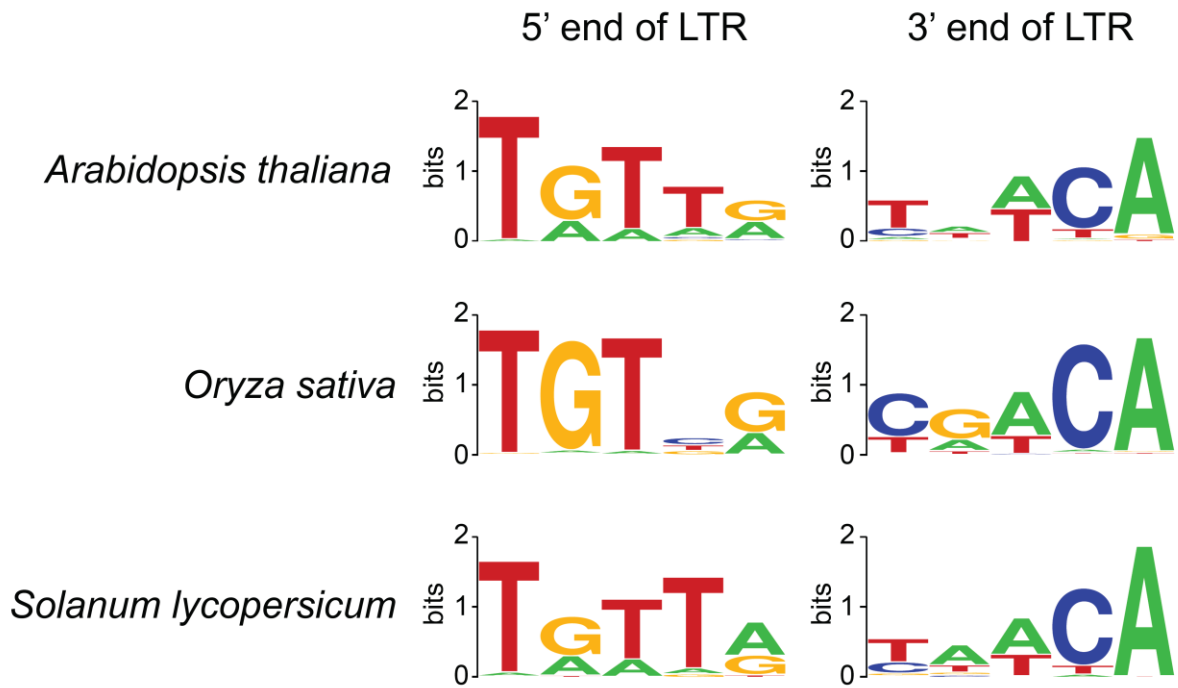
12

Supplementary Figure 3. ALE-seq detection of eclDNAs of *Arabidopsis* retrotransposons

Genome-wide plots (**a**, **b**, **d** and **f**) and read coverage plots (**c**, **e** and **g**) for ALE-seq profiles of *Arabidopsis* Col-0 wt (**a**), heat-stressed Col-0 (**b** and **c**), *met1-1* (**d** and **e**), and epi12 (**f** and **g**).
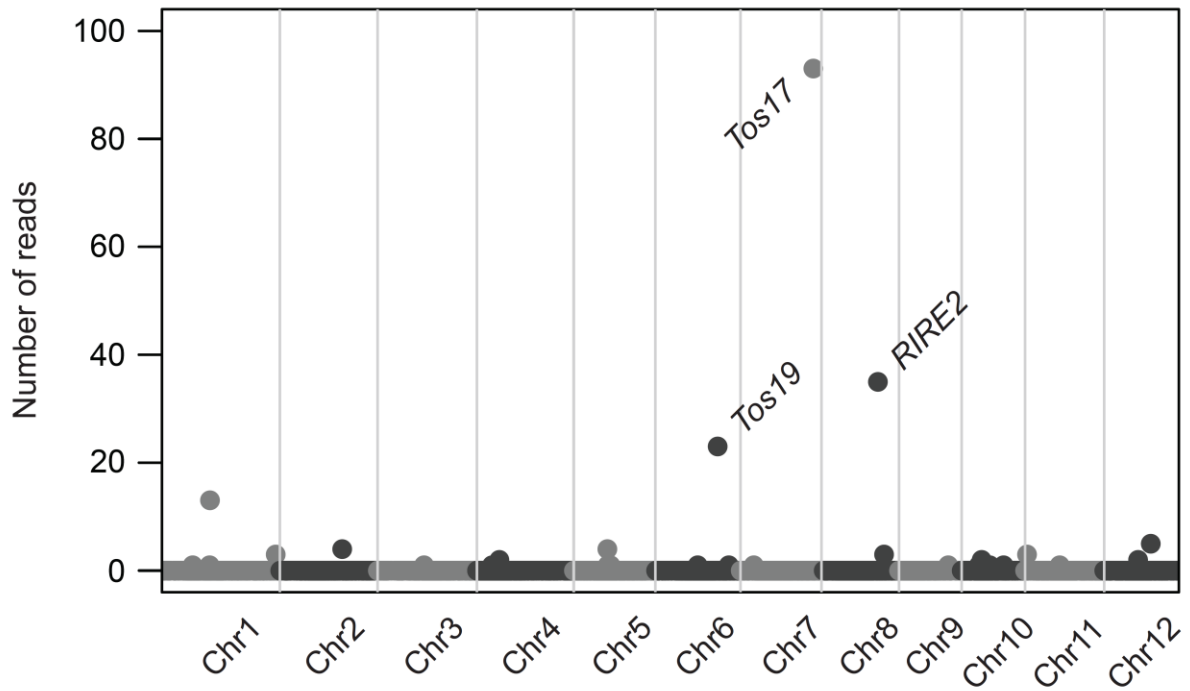
16

5' end of LTR   3' end of LTR

Arabidopsis thaliana

Oryza sativa

Solanum lycopersicum

Supplementary Figure 4. Conservation of end sequences of LTR

The conserved sequences of 5' and 3' ends of LTR. The first and last five nucleotides of LTRs

are displayed. The images were generated by the WebLogo tool
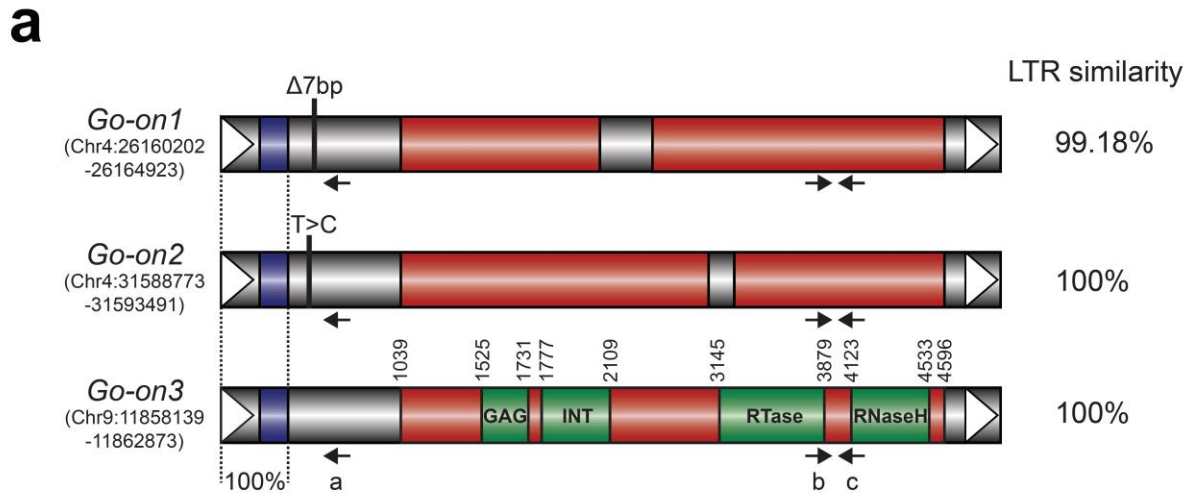
(http://weblogo.berkeley.edu/logo.cgi).

23

Supplementary Figure 5. ALE-seq detection of eclDNAs of rice retrotransposons using multiplexed PBS primers

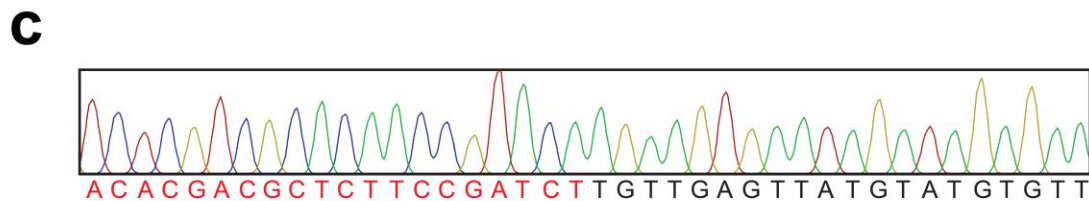Genome-wide plot for ALE-seq profiles of rice callus using pooled PBS primers of Met-iCAT and Arg-CCT.

Supplementary Figure 6. *Go-on* retrotransposon family

a, Schematic structure of *Go-on* retrotransposons. The genomic coordinates and LTR

similarities of each copy are shown at the left and right, respectively. Red boxes, ORFs;

green boxes, regions encoding protein domains; blue boxes, PBS; white arrowheads, LTRs.

Note that the sequences of the upstream LTRs through the PBS are identical in all three

copies. The sequence variation specific for each element is indicated. Protein domains were

predicted by NCBI BLASTP tool (https://blast.ncbi.nlm.nih.gov/Blast.cgi). Nucleotide

positions indicating the start and end of ORF and protein domains are provided. Primers

used for sequencing and qPCR analyses are shown as arrows. **b**, Multiple sequence

alignment of the genomic sequences of three *Go-on* copies and the sequenced ALE clones.

ALE-seq was performed using the RT primer specific to *Go-on3* indicated as "a" in **a**. The

41   resulting single-stranded first strand cDNA was PCR-amplified, cloned to the pGEM T-easy

42   vector, and sequenced. Multiple sequence alignment was performed by ClustalW

43   (http://www.genome.jp/tools-bin/clustalw) and visualized by boxshade tools

44   (https://www.ch.embnet.org/software/BOX_form.html). **c**, Sequencing of the ALE-seq

45   product of *Go-on3* showing the junction region of the adapter and LTR. Sequences in red

46   and black are the adapter and *Go-on* LTR, respectively.

47
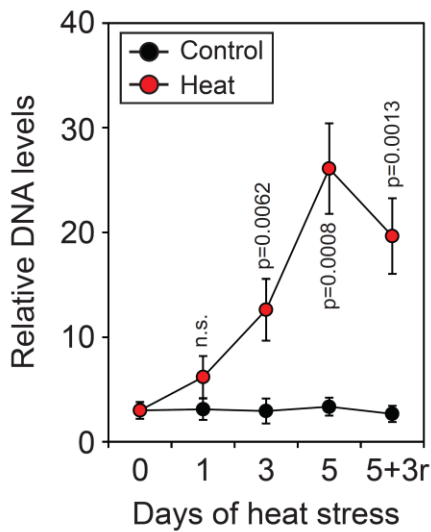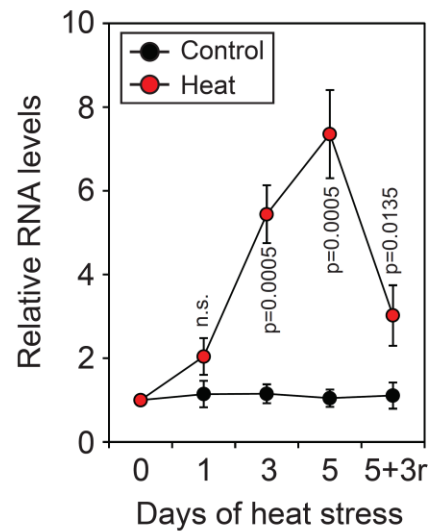
a and **b**, The relative levels of DNA (**a**) and RNA (**b**) of *Go-on3* determined by qPCR. Heat treatment (44°C) was applied to 1-week-old rice seedlings for the periods indicated; +3r means 3 days of recovery in normal growth conditions after heat stress. The levels are means ± sd of three biological replicates. For DNA analysis, Day 0 levels are set to 3, reflecting three genomic copies of *Go-on* in *japonica* rice. Normalization was done against *eEF1α*. P-values were calculated by a two-tailed Student's t-test; n.s., not significant. **c**, The sequence of the left LTR and PBS of *Go-on3*. The sequence in red is the heat-related HSFC1-binding sequence motif predicted by PlantPan 2.0 tool (http://plantpan2.itps.ncku.edu.tw/index.html) with statistically significant enrichment of *P*= 4.28e^{-10} as determined by Fisher's exact test. The enrichment of the sequence motif was

60   calculated by comparing the ten most similar sequences of *Go-on* found in rice genome with

61   1,000 random genomic loci of 150bp. The PBS is shown in blue.

62

63
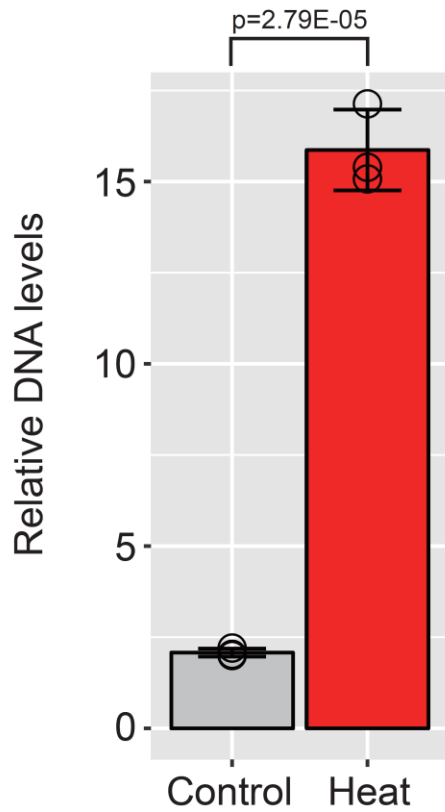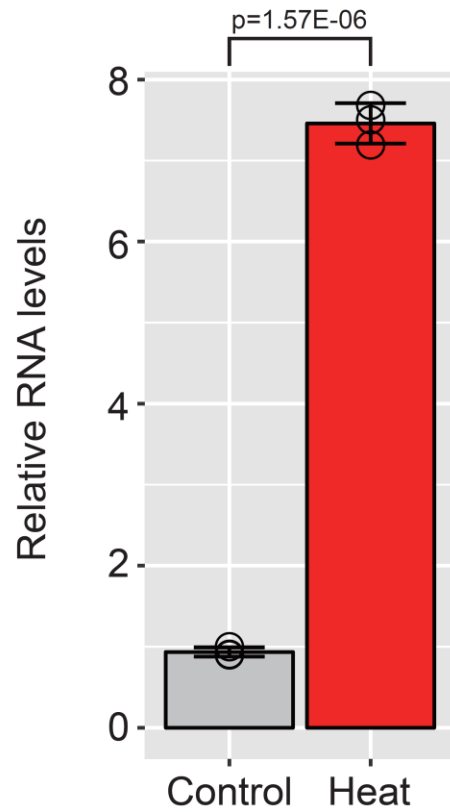
Supplementary Figure 8. Heat stress-triggered activation of *Go-on* in *indica* rice

a and **b**, The qPCR analyses for DNA (**a**) and RNA (**b**) levels of *Go-on* in *indica* rice. The levels are means ± sd of three biological replications. The levels of control sample are set to 2 (**a**) reflecting 2 genomic copies of *Go-on* in *indica* rice. P-values are determined by two-sided Student's t-test.

69

a, **b**

70
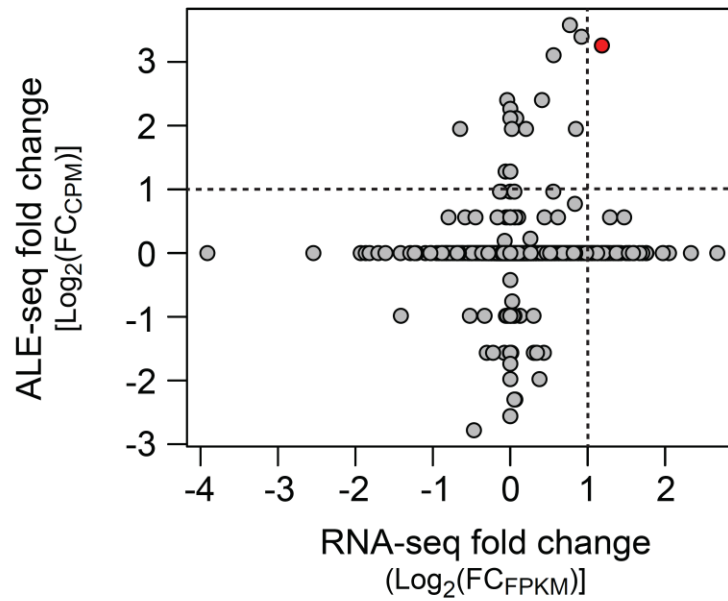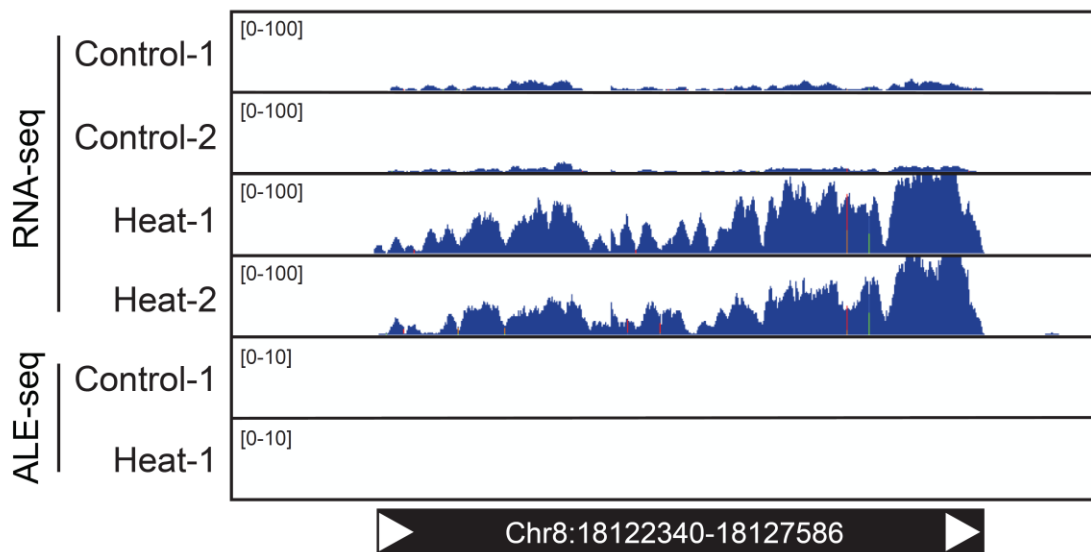
Supplementary Figure 9. Comparison of mRNA and eclDNA levels

a, Scatter plot for log2-fold changes (FCs) in RNA-seq and ALE-seq profiles in the control and heat-stressed rice plants used in Figure 3. FCs were calculated by dividing heat samples values by control samples values of CPM (counts per million reads) and FPKM (fragments per kb per million reads) for ALE-seq and RNA-seq data, respectively. Each dot represents an

76   individual retroelement and the dashed lines mark log2-FC one. Th retrotransposon in red

77   has log2-FC higher than one in both ALE-seq and RNA-seq. **b**, Read coverage plot for a

78   selected retrotransposon showing evidence of transcriptional activation upon heat stress

79   not followed by synthesis of eclDNAs.

80

81
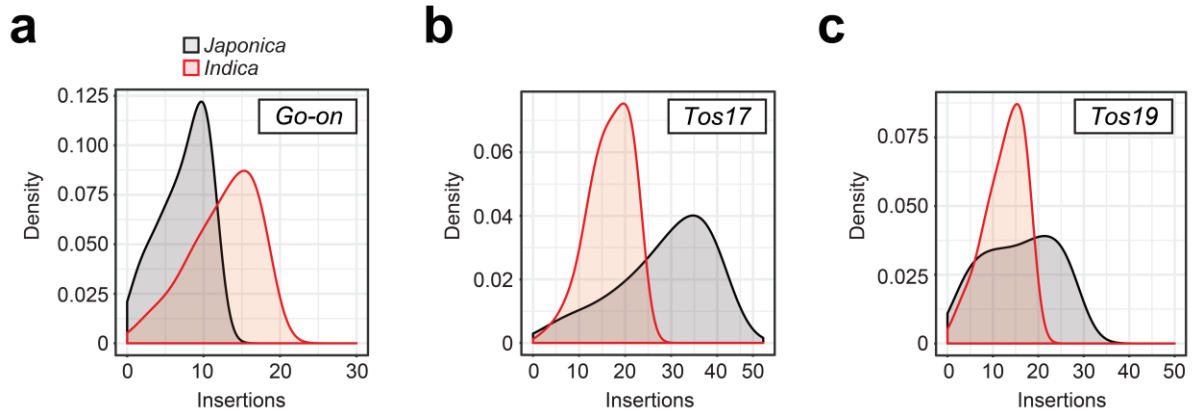
Supplementary Figure 10. Retrotransposon insertions in *japonica* and *indica* rice

a-**c**, Density plots for number of non-reference insertions in randomly selected 200 accessions out of 388 iterated by 1,000 times.

a

b

86
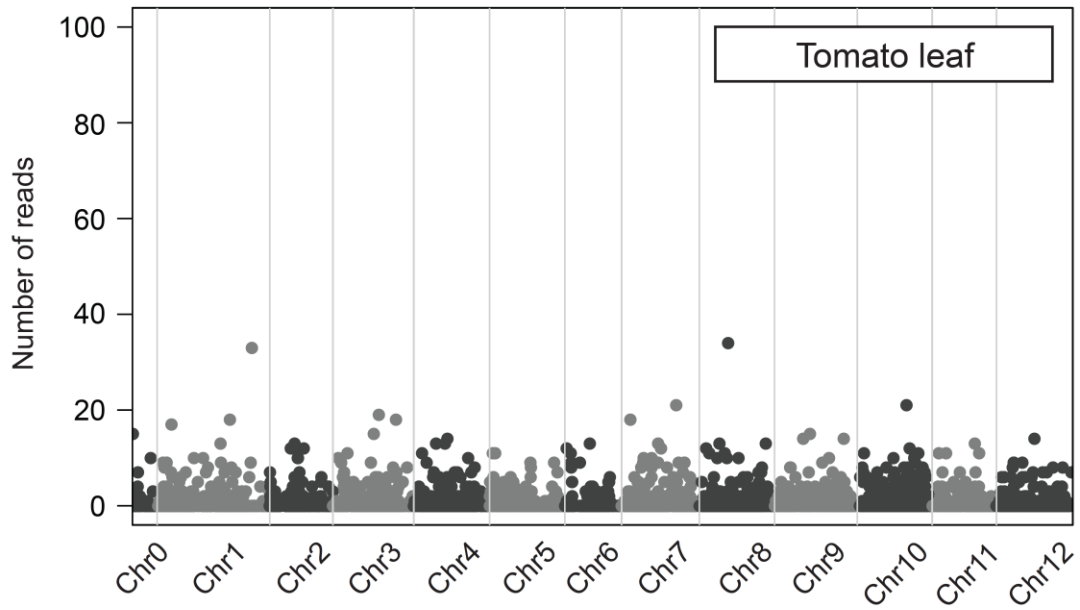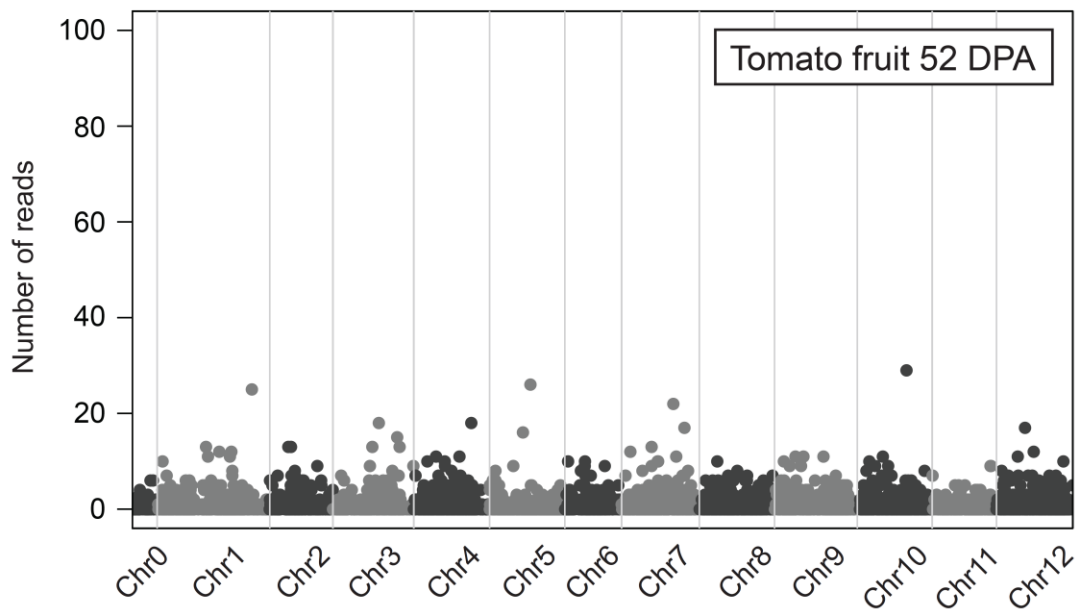
Supplementary Figure 11. ALE-seq profile of tomato leaves and fruits

a and **b**, Genome-wide plots for ALE-seq profiles performed in tomato leaves (**a**) and fruits
52 DPA (**b**). Each dot represents an individual retrotransposon.

90

91 **Supplementary Table 1.** Sequences of oligonucleotides used in this study

92 T7 promoter sequence is underlined and in bold is partial Illumina adapter sequence.

Primer	Sequence (5' → 3')
ALE adapter top strand	AGAGAG<u>TAATACGACTCACTATAGGG</u>**ACACGACGCTCTTCCGATCT**
ALE adapter bottom strand	**AGATCGGAAGAGCGTCGTGT**<u>CCCTATAGTGAGTCGTATTA</u>CTCTCT
ALE RT Met-iCAT-R	AGACGTGTGCTCTTCCGATCTGCTCTGATACCA
ALE RT Arg-CCT-R	AGACGTGTGCTCTTCCGATCTCCTGGCGCGCCA
ONSEN full length-F	TGTTGAAAGTTAAACTTGATTTTG
ONSEN full length-R	TGTTAGAGTAAAATTCTTTTAG
Go-on-F (b of Figure S5)	GGCAGAATACAGGGCAATGTC
Go-on-R (c of Figure S5)	GCCGACTTATTGTCACACCAC
Go-on RT-R (a of Figure S5)	TCTCTGCACGCCTCGACAAG
eEF1α-F	GCACGCTCTTCTTGCTTTCACTCT
eEF1α-R	AAAGGTCACCACCATACCAGGCTT
FIRE RT-F	GAGTTGGCTACGTATCGTTTGC
FIRE RT-R	AGCCTCCACAAATTCATCCCAT
FIRE copy number-F	GGTGTTCTCGTTGTGGTAAGT
FIRE copy number-R	TAAGGTGACACTCCCTCATAGT
SlCAC-F	CCTCCGTTGTGATGTAACTGG
SlCAC-R	ATTGGTGGAAAGTAACATCATCG
SlGAPDH-F	ATGCTCCCATGTTTGTTGTGGGTG
SlGAPDH-R	TTAGCCAAAGGTGCAAGGCAGTTC

93

94 **Supplementary Table 2.** Summary of ALE-seq libraries

95 Numbers of reads sequenced and mapped are summarised. Both unique-mappers and
96 multi-mappers are considered. "% mapped to LTRs" refers to all reads mapped throughout
97 retrotransposon.

Samples	Reads sequenced	% mapped to genome	% mapped to LTRs	% not mapped to LTRs	Accession number
Arabidopsis Col-0	56,057	93.20	17.77	75.43	SAMN09748167
Arabidopsis heat-stressed	45,554	90.33	15.85	74.48	SAMN09748168
Arabidopsis *met1-1*	58,029	94.79	16.03	78.76	SAMN09748169
Arabidopsis epi12	45,545	96.19	31.18	65.01	SAMN09748170
Rice leaf	27,063	97.54	12.33	85.21	SAMN09748171
Rice callus	25,183	95.67	13.58	82.09	SAMN09748172
Rice callus -Lig	37,610	83.48	11.75	71.73	SAMN09748173
Rice callus -T7	870	2.82	0.12	2.70	SAMN09748174
Rice callus -RT	516	1.26	0	1.26	SAMN09748175
Rice callus pooled PBS	22,939	90.06	14.16	75.90	SAMN09748176
Rice non-stressed	31,819	90.39	12.29	78.10	SAMN09748177
Rice heat-stressed	31,525	97.63	13.54	84.09	SAMN09748178
Tomato leaf	46,421	96.65	13.24	83.41	SAMN09748179
Tomato fruit 52 DPA	73,067	96.97	28.53	68.44	SAMN09748180

98

99   **Supplementary Table 3.** Non-reference insertions of *Go-on*.

100   Neo-insertions of *Go-on* detected by TIF. The positions are provided as coordinates of target
101   site duplication.

Chromosome	Start	End	Accession	Category
Chr4	31968290	31968294	ERS467756	*Indica*
Chr4	31968290	31968294	ERS467757	*Indica*
Chr1	43029985	43029989	ERS467791	*Indica*
Chr4	31968290	31968294	ERS467794	*Indica*
Chr4	31968290	31968294	ERS467830	*indica*
Chr1	43029985	43029989	ERS467831	*indica*
Chr4	31968290	31968294	ERS467831	*indica*
Chr7	29937784	29937788	ERS467843	*indica*
Chr1	43029985	43029989	ERS467872	*indica*
Chr4	31968290	31968294	ERS467876	*indica*
Chr1	43029985	43029989	ERS467877	*indica*
Chr1	43029985	43029989	ERS467878	*indica*
Chr8	5518300	5518306	ERS467878	*indica*
Chr7	29937784	29937788	ERS467880	*indica*
Chr4	31968290	31968294	ERS467883	*indica*
Chr11	1485949	1485953	ERS467910	*indica*
Chr1	43029985	43029989	ERS467915	*indica*
Chr4	31968290	31968294	ERS467924	*indica*
Chr7	29937784	29937788	ERS467925	*indica*
Chr4	31968290	31968294	ERS467926	*indica*
Chr1	20049396	20049400	ERS467927	*indica*
Chr8	5518300	5518306	ERS467934	*indica*
Chr1	43029985	43029989	ERS467938	*indica*
Chr1	20049396	20049400	ERS467943	*indica*
Chr8	3790507	3790511	ERS467943	*indica*
Chr1	20049396	20049400	ERS467944	*indica*
Chr4	31960603	31960607	ERS467952	*indica*
Chr8	5518300	5518306	ERS467952	*indica*
Chr8	5518300	5518306	ERS467959	*indica*
Chr1	20049396	20049400	ERS467960	*indica*
Chr1	43029985	43029989	ERS467961	*indica*
Chr1	20049396	20049400	ERS467962	*indica*
Chr4	13737528	13737532	ERS467962	*indica*
Chr7	29937784	29937788	ERS467962	*indica*
Chr1	43029985	43029989	ERS467966	*indica*
Chr1	43029985	43029989	ERS467969	*indica*
Chr4	31968290	31968294	ERS467969	*indica*
Chr1	43029985	43029989	ERS467979	*indica*
Chr8	5518300	5518306	ERS467980	*indica*
Chr1	43029985	43029989	ERS467986	*indica*
Chr4	31968290	31968294	ERS467995	*indica*
Chr7	29937784	29937788	ERS467995	*indica*
Chr12	16846383	16846387	ERS467996	*indica*
Chr4	31968290	31968294	ERS467996	*indica*
Chr8	5518300	5518306	ERS467996	*indica*
Chr5	287377	287381	ERS467998	*indica*
Chr1	43029985	43029989	ERS467999	*indica*
Chr8	3790507	3790511	ERS468001	*indica*
Chr1	20049396	20049400	ERS468004	*indica*
Chr8	5518300	5518306	ERS468004	*indica*
Chr1	20049396	20049400	ERS468006	*indica*
Chr8	5518300	5518306	ERS468006	*indica*
Chr4	31960603	31960607	ERS468008	*indica*
Chr7	29937784	29937788	ERS468011	*indica*

Chr8	5518300	5518306	ERS468011	*indica*
Chr1	43029985	43029989	ERS468014	*indica*
Chr12	16846383	16846387	ERS468016	*indica*
Chr4	31960603	31960607	ERS468018	*indica*
Chr1	43029985	43029989	ERS468023	*indica*
Chr1	43029985	43029989	ERS468025	*indica*
Chr8	5518299	5518306	ERS468028	*indica*
Chr1	43029985	43029989	ERS468029	*indica*
Chr4	31968290	31968294	ERS468042	*indica*
Chr7	29937784	29937788	ERS468048	*indica*
Chr1	43029985	43029989	ERS468049	*indica*
Chr8	5518300	5518306	ERS468050	*indica*
Chr1	43029985	43029989	ERS468052	*indica*
Chr8	5518300	5518306	ERS468053	*indica*
Chr4	13737528	13737532	ERS468055	*indica*
Chr8	5518300	5518306	ERS468055	*indica*
Chr7	29937784	29937788	ERS468059	*indica*
Chr7	29937784	29937788	ERS468060	*indica*
Chr6	31319589	31319593	ERS468065	*indica*
Chr1	43029985	43029989	ERS468066	*indica*
Chr4	13737528	13737532	ERS468068	*indica*
Chr8	5518300	5518306	ERS468071	*indica*
Chr1	20049396	20049400	ERS468072	*indica*
Chr7	29937784	29937788	ERS468073	*indica*
Chr4	31968290	31968294	ERS468074	*indica*
Chr4	31960603	31960607	ERS468075	*indica*
Chr12	16846383	16846387	ERS468077	*indica*
Chr1	20049396	20049400	ERS468078	*indica*
Chr8	5518300	5518306	ERS468084	*indica*
Chr11	29783248	29783252	ERS468086	*indica*
Chr1	20049396	20049400	ERS468087	*indica*
Chr1	20049396	20049400	ERS468088	*indica*
Chr8	5518300	5518306	ERS468088	*indica*
Chr8	5518300	5518306	ERS468089	*indica*
Chr12	22672020	22672024	ERS468095	*indica*
Chr4	31960603	31960607	ERS468101	*indica*
Chr1	43029985	43029989	ERS468102	*indica*
Chr1	43029985	43029989	ERS468104	*indica*
Chr4	31968290	31968294	ERS468106	*indica*
Chr12	16846383	16846387	ERS468111	*indica*
Chr1	43029985	43029989	ERS468112	*indica*
Chr1	43029985	43029989	ERS468115	*indica*
Chr8	5518300	5518306	ERS468121	*indica*
Chr4	31968290	31968294	ERS468126	*indica*
Chr8	5518300	5518306	ERS468131	*indica*
Chr8	5518300	5518306	ERS468133	*indica*
Chr1	20049396	20049400	ERS468134	*indica*
Chr4	31968290	31968294	ERS468136	*indica*
Chr1	43029985	43029989	ERS468138	*indica*
Chr4	31968290	31968294	ERS468139	*indica*
Chr8	5518300	5518306	ERS468142	*indica*
Chr4	31968290	31968294	ERS468154	*indica*
Chr4	31968290	31968294	ERS468157	*indica*
Chr1	43029985	43029989	ERS468160	*indica*
Chr1	43029985	43029989	ERS468161	*indica*
Chr4	31968290	31968294	ERS468163	*indica*
Chr1	20049396	20049400	ERS468166	*indica*
Chr4	31968290	31968294	ERS468169	*indica*
Chr5	19524953	19524957	ERS468170	*indica*
Chr4	31968290	31968294	ERS468174	*indica*
Chr8	5518300	5518306	ERS468184	*indica*

Chr8	5518300	5518306	ERS468186	*indica*
Chr4	31968290	31968294	ERS468187	*indica*
Chr8	5518300	5518306	ERS468187	*indica*
Chr4	31968290	31968294	ERS468191	*indica*
Chr4	31968290	31968294	ERS468192	*indica*
Chr4	31968290	31968294	ERS468193	*indica*
Chr8	5518300	5518306	ERS468195	*indica*
Chr4	31968290	31968294	ERS468202	*indica*
Chr7	29937784	29937788	ERS468202	*indica*
Chr4	31968290	31968294	ERS468204	*indica*
Chr4	31968290	31968294	ERS468205	*indica*
Chr8	5518300	5518306	ERS468207	*indica*
Chr8	5518300	5518306	ERS468209	*indica*
Chr7	29937784	29937788	ERS468210	*indica*
Chr11	30168035	30168039	ERS468212	*indica*
Chr5	287377	287381	ERS468212	*indica*
Chr1	43029985	43029989	ERS468215	*indica*
Chr4	31968290	31968294	ERS468222	*indica*
Chr4	31968290	31968294	ERS468230	*indica*
Chr4	31968290	31968294	ERS468232	*indica*
Chr4	31968290	31968294	ERS468234	*indica*
Chr1	43029985	43029989	ERS468237	*indica*
Chr4	13737528	13737532	ERS468240	*indica*
Chr7	29937784	29937788	ERS468249	*indica*
Chr1	43029985	43029989	ERS468250	*indica*
Chr3	431859	431863	ERS468252	*indica*
Chr7	29937784	29937788	ERS468252	*indica*
Chr11	29783248	29783252	ERS468255	*indica*
Chr1	19257271	19257275	ERS467801	*japonica*
Chr5	23638163	23638167	ERS467889	*japonica*
Chr11	1514174	1514178	ERS467893	*japonica*
Chr8	5635769	5635774	ERS467904	*japonica*
Chr11	1514174	1514178	ERS468026	*japonica*
Chr5	258622	258626	ERS468308	*japonica*
Chr8	5635768	5635774	ERS468310	*japonica*
Chr1	41968356	41968360	ERS468380	*japonica*
Chr8	5635768	5635774	ERS468383	*japonica*
Chr8	5635768	5635774	ERS468384	*japonica*
Chr8	5635768	5635774	ERS468387	*japonica*
Chr8	5635768	5635774	ERS468402	*japonica*
Chr6	24954457	24954461	ERS468442	*japonica*
Chr6	22413483	22413487	ERS468446	*japonica*
Chr7	29379081	29379085	ERS468449	*japonica*
Chr8	5635769	5635774	ERS468449	*japonica*
Chr8	5635768	5635774	ERS468456	*japonica*
Chr8	5635768	5635774	ERS468458	*japonica*
Chr8	5635769	5635774	ERS468595	*japonica*
Chr8	5635768	5635774	ERS468596	*japonica*
Chr8	5635768	5635774	ERS468604	*japonica*
Chr8	5635768	5635774	ERS468613	*japonica*
Chr8	5635768	5635775	ERS468617	*japonica*
Chr8	5635768	5635774	ERS468620	*japonica*
Chr6	22413483	22413487	ERS468649	*japonica*
Chr5	258622	258626	ERS468684	*japonica*
Chr7	29379081	29379085	ERS468704	*japonica*
Chr8	5635768	5635774	ERS468705	*japonica*
Chr5	258622	258626	ERS468721	*japonica*
Chr5	23638163	23638167	ERS468734	*japonica*
Chr1	41968356	41968360	ERS468902	*japonica*
Chr1	41968356	41968360	ERS468917	*japonica*
Chr8	5635769	5635774	ERS468993	*japonica*

Chr2	1659944	1659948	ERS469049	*japonica*
Chr8	5635768	5635774	ERS469069	*japonica*
Chr8	5635768	5635774	ERS469132	*japonica*
Chr8	5635768	5635774	ERS469177	*japonica*
Chr8	5635768	5635774	ERS469199	*japonica*
Chr8	5635768	5635774	ERS469215	*japonica*
Chr8	5635768	5635774	ERS469302	*japonica*
Chr8	5635768	5635774	ERS469307	*japonica*
Chr8	5635768	5635774	ERS469556	*japonica*
Chr8	5635768	5635774	ERS469602	*japonica*
Chr8	5635768	5635774	ERS469604	*japonica*
Chr8	5635768	5635774	ERS469605	*japonica*
Chr8	5635768	5635775	ERS469637	*japonica*
Chr8	5635768	5635774	ERS469650	*japonica*
Chr8	5635768	5635774	ERS469668	*japonica*
Chr8	5635768	5635774	ERS469669	*japonica*
Chr8	5635768	5635774	ERS469689	*japonica*
Chr8	5635768	5635774	ERS469694	*japonica*
Chr8	5635768	5635774	ERS469696	*japonica*
Chr8	5635768	5635774	ERS469699	*japonica*
Chr8	5635768	5635774	ERS469746	*japonica*
Chr8	5635768	5635774	ERS469758	*japonica*
Chr8	5635768	5635774	ERS469845	*japonica*
Chr8	5635768	5635774	ERS469880	*japonica*
Chr8	5635768	5635774	ERS469978	*japonica*
Chr8	5635768	5635774	ERS469985	*japonica*
Chr8	5635768	5635774	ERS470129	*japonica*
Chr8	5635768	5635774	ERS470132	*japonica*
Chr8	5635768	5635774	ERS470188	*japonica*
Chr8	5635768	5635774	ERS470344	*japonica*
Chr8	5635768	5635774	ERS470439	*japonica*
Chr8	5635768	5635774	ERS470516	*japonica*